Interaction Notes

Note 315

December 1976

EMP Penetration through Advanced Composite Skin Panels

K.F. Casey

EMtec, Inc.
1100 Glendon Avenue
Los Angeles, California 90024

Abstract

Simple analytical models are developed and analyzed to yield electromagnetic characterizations of advanced composite skin panels over the EMP frequency range. The panels are modeled as uniaxially anisotropic slabs whose optic axes are oriented normal to the slab boundaries. Graphite composite panels are modeled as anisotropic conducting media and boron-epoxy panels as anisotropic dielectric media. The relevant conductivities and permittivities are estimated in terms of the configuration and electrical properties of the fibers and the epoxy matrix. An equivalent sheet impedance is derived to characterize the wire mesh screen which is often embedded in one surface of a boron-epoxy panel in order to improve its electromagnetic shielding effectiveness. It is shown that the most important parameters for characterizing composite skin panels are the transverse conductivity of graphite composite and the screen parameters and geometric mean of the transverse and longitudinal permittivities for screened boron-epoxy composites.

I. INTRODUCTION

Aircraft skin panels made of advanced composite materials have a significant advantage in weight savings over metallic (e.g., aluminum or titanium) panels, but advanced composites differ substantially from metals in their electrical properties. The differences are generally unfavorable from the standpoint of electromagnetic shielding effectiveness; consequently, the study of electromagnetic field penetration through advanced composite materials assumes a special importance.

A panel of advanced composite material is a laminate, made up of several individual laminae or thin sheets which have been bonded together. Each lamina consists of a one-dimensional array of fibers embedded in an epoxy matrix. The fibers are graphite† (a mediocre conductor) in "graphite" composites, or boron (a poor dielectric) in "boron-epoxy" composites. A typical lamina is depicted in Fig. (1). The laminate is made by laying up several laminae in one of several possible configurations, perhaps the most common of which is the 0°-90° layup shown in Fig. (2), in which the fibers in alternate laminae are oriented at right angles to each other. This layup is then cured to bond the laminae together and thus form the final product.

Since the boron-epoxy composites are poor conductors, a wire mesh screen is sometimes embedded in one surface of the laminate before it is cured, in order to improve its shielding effectiveness. Such a "screened" boron-epoxy composite laminate is shown in Fig. (3). In this Memo we shall be concerned with unscreened graphite and screened boron-epoxy composite laminates.

The electrical properties of advanced composite materials have not yet been well studied [1]. In fact, much of the data which are now available have been inferred from shielding measurements and have not been obtained directly. In the absence of reliable values for such parameters as the mean conductivity and permittivity†† for a panel, we shall attempt insofar as possible to formulate approximate descriptions of advanced composite materials which do

†i.e., a pyrolyzed organic fiber such as polyacrylonitrile.

††all the constituent materials of typical laminates are non-magnetic (relative permeability = 1), so the laminates themselves are essentially non-magnetic.

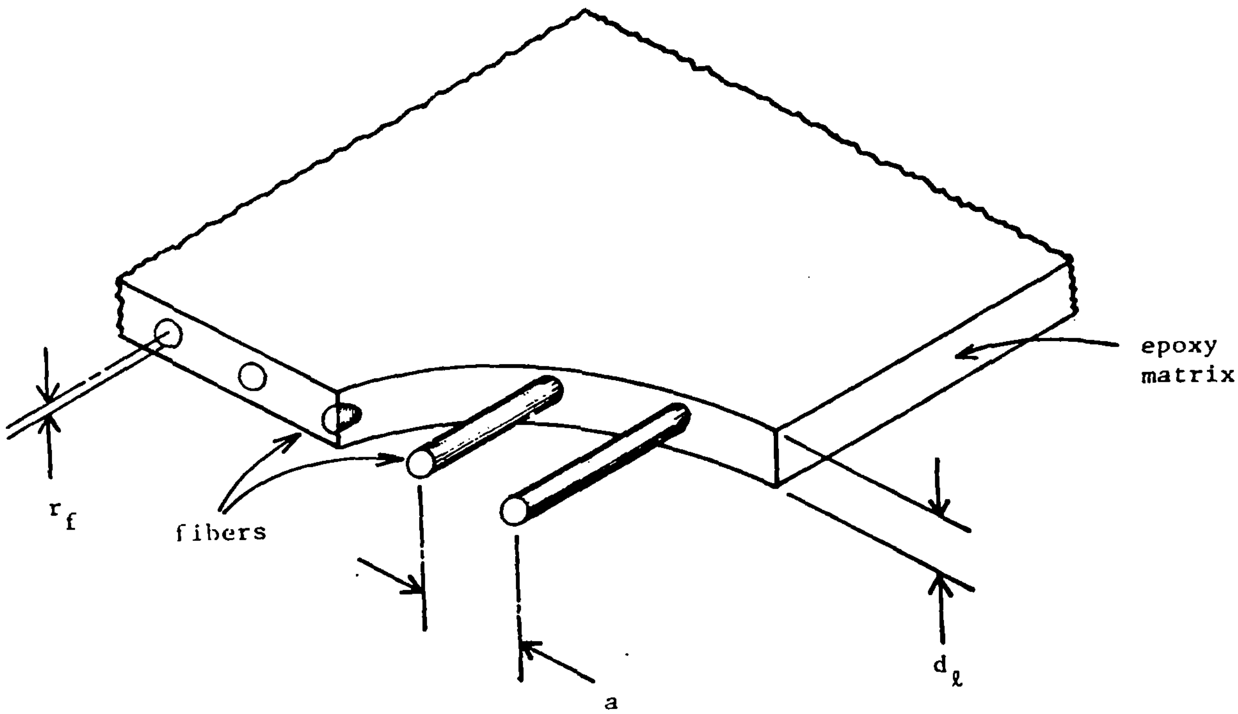

Fig. 1. A lamina of advanced composite.

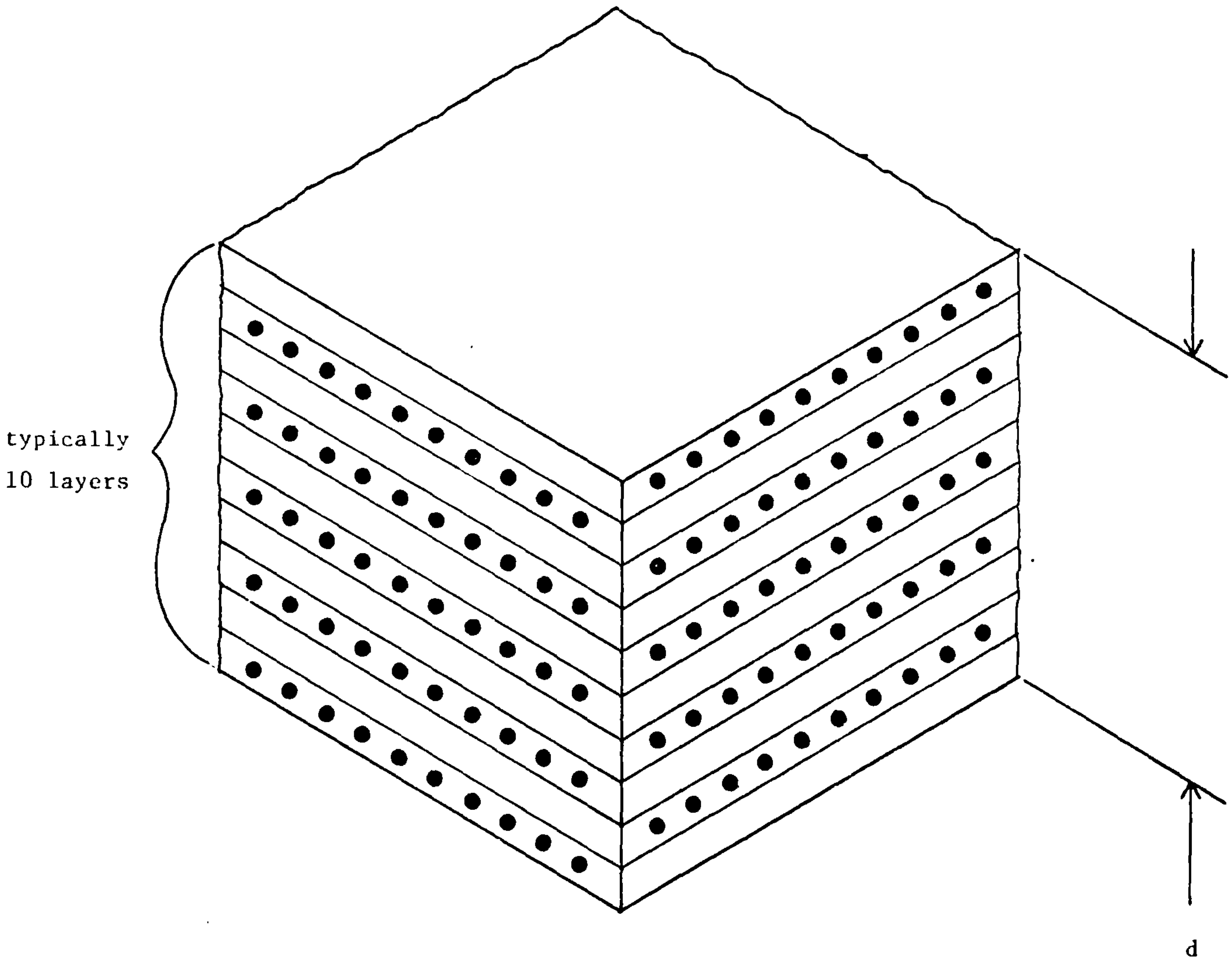

Fig. 2. 0° - 90° layup for a laminate panel.

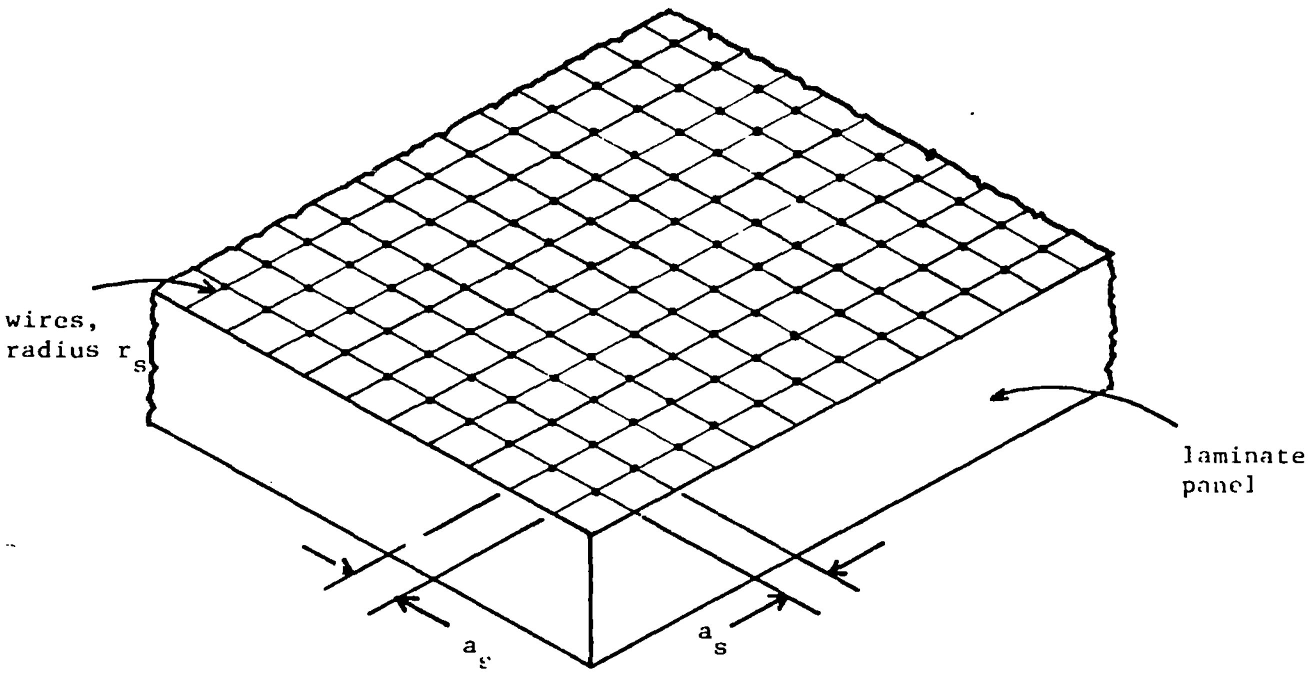

Fig. 3. A screened laminate. The wire mesh is square and junctions are assumed to be bonded.

not require that the exact values of these parameters be known in order to be useful.

In the next section, we describe a set of theoretical models and boundary-value problems relevant to the analysis of EMP penetration of advanced composite panels. These models and problems are studied in Section III. The results are summarized and discussed, and illustrated with numerical examples, in Section IV.

II. THEORETICAL MODELS AND PROBLEMS

In developing analytical models for advanced composite skin panels we shall confine our attention to planar geometry. Consideration of planar problems for developing electromagnetic characterizations of these materials is justified because of the following facts:

1. advanced composite materials of the types we shall consider are lossy, and the wavelength of a monochromatic field inside the material is smaller than that outside; furthermore,
2. in practical configurations, the thickness of the laminate is small in comparison to either of its local principal radii of curvature.

We infer from the first of these observations that the electromagnetic behavior of the laminate is essentially a local phenomenon, in that the fields at two points in the laminate are not closely coupled if the separation of the two points greatly exceeds the panel thickness. Thus the development of a "transfer characteristic" for a laminate panel does not require consideration of the panel as a whole, but only of relatively small local portions of it. By virtue of the second observation above, these local portions can be considered to be planar.

A. Model for a Single Lamina

A single lamina is shown in Fig. (1). Such a lamina is typically 0.25 mm thick and the volume fraction occupied by the fibers is typically 25-50%. Over the EMP frequency range, the lamina is electrically very thin; furthermore, the fiber separation is a very small fraction of a wavelength. The lamina will therefore be modeled electromagnetically by a thin layer of anisotropic material. Let us define "lamina coordinates" (ξ_1,ξ_2,ξ_3) such that ξ_1 is the coordinate direction parallel to the fibers, ξ_2 is the direction normal to the fiber axes but parallel to the lamina surface, and ξ_3 is the direction normal to the lamina. Then if $\overline{\overline{\sigma}}_\ell$ and $\overline{\overline{\varepsilon}}_\ell$ denote the conductivity and permittivity dyadics of the lamina, we have

$$\overline{\overline{\sigma}}_\ell + s\overline{\overline{\varepsilon}}_\ell = \sum_{i=1}^{3} (\sigma_{\ell i} + s\varepsilon_{\ell i})\bar{a}_{\xi i}\bar{a}_{\xi i} \tag{1}$$

where $\bar{a}_{\xi i}$ is the unit vector in the positive ξ_i-direction and s denotes the complex frequency: the electromagnetic field is assumed to vary with time as exp(st). The parameters $\sigma_{\ell i}$ and $\varepsilon_{\ell i}$ are the conductivity and permittivity in the ξ_i direction. These quantities can be determined experimentally or calculated from appropriately chosen boundary-value problems. The justification for this characterization of the lamina, in which the details of the interior structure are effectively ignored, lies in the fact that the relevant dimensions are all extremely small in comparison to the wavelength. Thus the spatial periodicity of the structure is unimportant except in the actual calculation of $\sigma_{\ell i}$ and $\varepsilon_{\ell i}$.

A.1. Graphite laminae

The conductivity of the epoxy matrix is negligible, and we shall assume that the graphite fibers in a graphite composite lamina are effectively insulated from each other. Thus we may set the transverse conductivities $\sigma_{\ell 2}$ and $\sigma_{\ell 3}$ equal to zero. Additionally, we assume that in the frequency range of interest, $\sigma_{\ell 1} >> |s\varepsilon_{\ell 1}|$ so that the lamina acts as a good conductor along the fiber-axis direction ξ_1†. Therefore, for a single lamina of graphite composite,

$$\bar{\bar{\sigma}}_\ell + s\bar{\bar{\varepsilon}}_\ell \simeq \sigma_{\ell 1}\bar{a}_{\xi 1}\bar{a}_{\xi 1} + s\sum_{i=2}^{3}\varepsilon_{\ell i}\bar{a}_{\xi i}\bar{a}_{\xi i} \qquad (2)$$

A.2. Boron-epoxy laminae

Neither the boron tungstate fibers nor the epoxy matrix are conductors, so $\sigma_{\ell i} = 0$ (i = 1,2,3). Thus for a boron-epoxy composite lamina

$$\bar{\bar{\sigma}}_\ell = \bar{\bar{0}} \qquad (3a)$$

$$\bar{\bar{\varepsilon}}_\ell = \sum_{i=1}^{3}\varepsilon_{\ell i}\bar{a}_{\xi i}\bar{a}_{\xi i} \qquad (3b)$$

---

†i.e., in that the displacement current density is negligible in comparison to the conduction current density in the ξ_1-direction.

A.3. Analytical model for the determination of $\sigma_{\ell 1}$ and $\epsilon_{\ell i}$ $(i = 1,2,3)$

The structure to be analyzed to yield the constitutive parameters $\sigma_{\ell 1}$, $\epsilon_{\ell i}$ $(i = 1,2,3)$ is shown in Fig. (4). This model is a one-dimensional array of dielectric or conducting cylinders of radius r_f in an infinite medium of permittivity ϵ_m. The element spacing is a. The lamina itself is the region $|\xi_3| \leq d_\ell/2$. We shall consider only dipole interactions in the determination of $\epsilon_{\ell 2}$ and $\epsilon_{\ell 3}$. This procedure is strictly valid only when r_f is small in comparison to a; this is not necessarily the case in the present problem. However, the results will suffice for our purposes. This model is analyzed in Section III,A.

B. Model for a Laminate

For 0°-90° layup (or for other layup configurations in which there is no net preferred fiber orientation), a laminate model is readily obtained from a simple field averaging over pairs of laminae. This procedure is justified if the laminae are electrically very thin as we have assumed, and if the reactive field of the periodic fiber array of a single lamina does not significantly affect adjacent laminae. This latter assumption is readily justified: when the fiber separation is small in comparison to the wavelength, the reactive field decays in the directions normal to the lamina as $\exp(-2\pi|\xi_3|/a)$, where a is the fiber separation. Thus if d_ℓ is the thickness of a single lamina, we require that $\exp(-2\pi d_\ell/a)$ be small in comparison to unity. Typical values for d_ℓ/a are in the neighborhood of unity, so that $\exp(-2\pi d_\ell/a)$ is typically of order 10^{-3}; therefore the reactive-field interaction between adjacent laminae may be neglected.

An electromagnetic model for a laminate is a slab of uniaxially anisotropic material. Denoting its conductivity and permittivity dyadics by $\overline{\overline{\sigma}}_L$ and $\overline{\overline{\epsilon}}_L$, we readily obtain by simple averaging of the fields over adjacent laminae

$$\overline{\overline{\sigma}}_L + s\overline{\overline{\epsilon}}_L = \frac{1}{2}\left[(\sigma_{\ell 1} + \sigma_{\ell 2}) + s(\epsilon_{\ell 1} + \epsilon_{\ell 2})\right](\bar{a}_{\xi 1}\bar{a}_{\xi 1} + \bar{a}_{\xi 2}\bar{a}_{\xi 2})$$
$$+ (\sigma_{\ell 3} + s\epsilon_{\ell 3})\bar{a}_{\xi 3}\bar{a}_{\xi 3} \qquad (4)$$

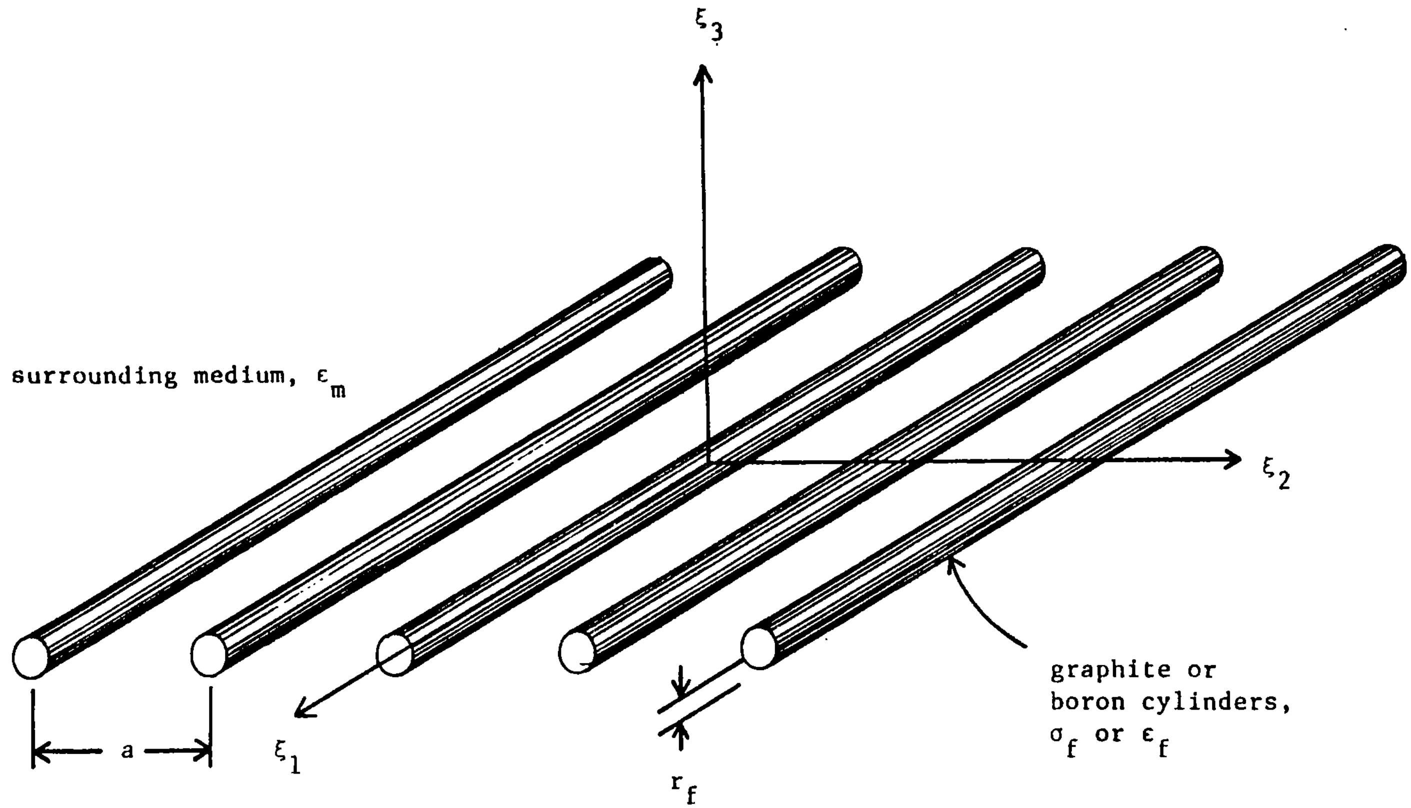

Fig. 4. Structure for the analytical determination of constitutive parameters.

For the special cases of graphite and boron-epoxy composites, we obtain from eqs. (2)-(4)

<u>graphite</u>: $$\bar{\bar{\sigma}}_L + s\bar{\bar{\epsilon}}_L \simeq \frac{1}{2}\sigma_{\ell 1}(\bar{a}_{\xi 1}\bar{a}_{\xi 1} + \bar{a}_{\xi 2}\bar{a}_{\xi 2}) + s\epsilon_{\ell 3}\bar{a}_{\xi 3}\bar{a}_{\xi 3} \qquad (5)$$

<u>boron-epoxy</u>: $$\bar{\bar{\sigma}}_L = \bar{\bar{0}} \qquad (6a)$$

$$\bar{\bar{\epsilon}}_L = \frac{1}{2}(\epsilon_{\ell 1} + \epsilon_{\ell 2})(\bar{a}_{\xi 1}\bar{a}_{\xi 1} + \bar{a}_{\xi 2}\bar{a}_{\xi 2}) + \epsilon_{\ell 3}\bar{a}_{\xi 3}\bar{a}_{\xi 3} \qquad (6b)$$

Thus the graphite composite laminate is modeled as a transversely conducting slab, and the boron-epoxy composite laminate is modeled as a slab of uniaxially anisotropic dielectric, the optic axis being normal to the slab boundaries in each case.

C. Wire-mesh Screen Model

The wire-mesh screen configuration has been shown in Fig. (3). The wire radii r_s are small in comparison to the square-mesh period a_s, and the junctions are assumed to be bonded. The assumption that $r_s \ll a_s$ is not always satisfied for real screens; however, it will produce a conservative estimate for the equivalent sheet admittance. The wire spacing a_s will be assumed small in comparison to the wavelengths in free space and in the laminate; we shall also assume that the wire spacing is less than or equal to the laminate thickness. This latter assumption, which is satisfied in practice, allows us to neglect the finite thickness of the laminate in determining the equivalent sheet impedance of the screen, since the reactive field carried by the screen will not penetrate through the laminate.

The wires themselves are characterized by their impedance per unit length, given by

$$Z_w = \frac{(s\mu_o/\sigma_w)^{1/2}}{2\pi r_s} \frac{I_o(\sqrt{s\mu_o\sigma_w}\, r_s)}{I_1(\sqrt{s\mu_o\sigma_w}\, r_s)} \qquad (7)$$

in which σ_w denotes the wire conductivity. $I_n(\cdot)$ denotes the modified Bessel function of the first kind of order n. The screen wires are non-magnetic ($\mu_r = 1$); the wires are typically made of aluminum.

D. Electromagnetic Boundary-Value Problems

We address several electromagnetic boundary-value problems in the next section. These include:

D.1. Determination of $\sigma_{\ell 1}$ (or $\varepsilon_{\ell 1}$), $\varepsilon_{\ell 2}$ and $\varepsilon_{\ell 3}$ for a composite lamina: the geometry of this problem is shown in Fig. (4). We consider the application of a uniform electric field $E_o\bar{a}_{\xi i}$ ($i = 1,2,3$) and using standard techniques determine the resulting polarizations or current density. These results are used to evaluate the constitutive parameters of the lamina.

D.2. EMP penetration of a graphite composite panel: the geometry for this problem is shown in Fig. (5). We consider the reflection and transmission of a plane electromagnetic wave by a planar layer of transversely conducting material. The results of this analysis yield a relatively simple matrix description of the field transfer characteristic of the panel.

D.3. EMP penetration of a screened boron-epoxy composite panel: the geometry of this problem is shown in Fig. (6). The panel is modeled as an anisotropic dielectric slab with a screen in one surface. The screen is modeled by an equivalent sheet admittance. We consider the reflection and transmission of a plane electromagnetic wave by the screen-slab configuration.

D.4. Evaluation of the equivalent sheet impedance of a bonded wire screen in a dielectric interface: the screen geometry has been shown in Fig. (3). The screen is located in the interface between two homogeneous dielectric half-spaces. The boron-epoxy composite laminate is modeled as a uniaxially isotropic medium.

The results of these analyses will be summarized, discussed, and illustrated in Section IV.

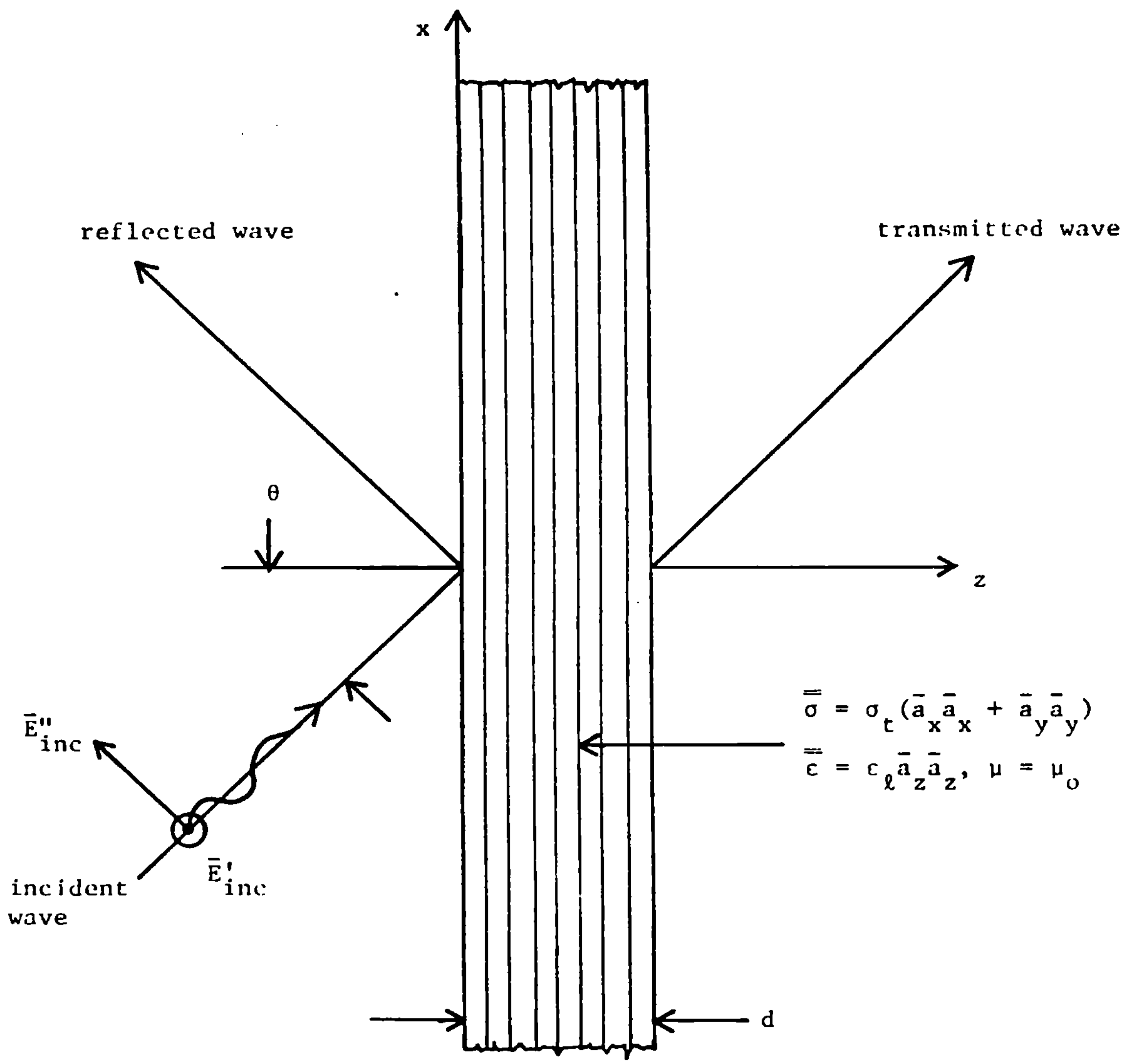

Fig. 5. Geometry for analysis of EMP penetration of graphite composite panel. The medium outside the panel is free space.

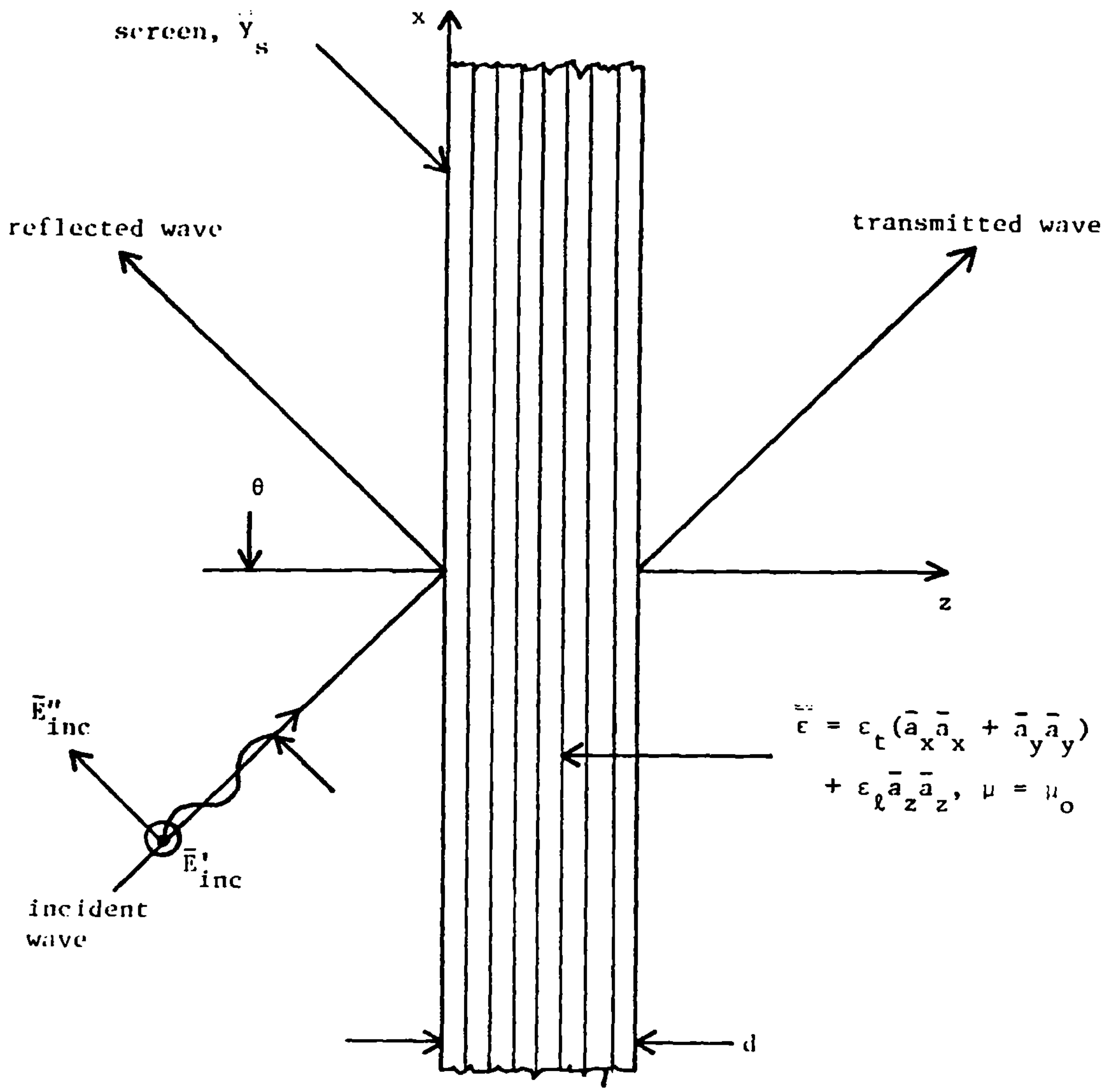

Fig. 6. Geometry for analysis of EMP penetration of screened boron-epoxy composite panel. The medium outside the panel is free space.

III. ANALYSIS OF PROBLEMS

Before proceeding to the analysis of the boundary-value problems which have been described in the preceding, we develop a "boundary connection operator" which relates the fields on one side of a planar layer of material to those on the other side. This "transfer function" operator formulation will be useful in dealing with the reflection and transmission problems to be addressed in Sections III,B and C.

The relation between the fields on either side of a uniaxially anisotropic shield of general type† is best developed in terms of the Fourier spatial spectra of the electric and magnetic fields $\bar{E}$ and $\bar{H}$. Thus we write

$$\begin{bmatrix} \bar{E}(\xi_1,\xi_2,\xi_3) \\ \\ \bar{H}(\xi_1,\xi_2,\xi_3) \end{bmatrix} = \int_{-\infty}^{\infty}\int_{-\infty}^{\infty} \begin{bmatrix} \tilde{\bar{E}}(\bar{k}_t,\xi_3) \\ \\ \tilde{\bar{H}}(\bar{k}_t,\xi_3) \end{bmatrix} e^{-j\bar{k}_t\cdot\bar{r}}\, d^2\bar{k}_t \tag{8}$$

in which $\tilde{\bar{E}}$ and $\tilde{\bar{H}}$ denote the Fourier spectra of $\bar{E}$ and $\bar{H}$, $\bar{r}$ is the position vector, and $\bar{k}_t$ is the Fourier spectral variable; furthermore, $\bar{k}_t\cdot\bar{a}_{\xi 3} = 0$.

It is convenient to work with the perpendicular- and parallel-polarized components of $\tilde{\bar{E}}$ and $\tilde{\bar{H}}$ separately. The perpendicular-polarized part of the electromagnetic field is derivable from a function $\tilde{\Phi}(\xi_3)$ as follows:

$$\tilde{\bar{E}}' = -j\bar{k}_t \times \bar{a}_{\xi 3}\tilde{\Phi} \tag{9a}$$

$$\tilde{\bar{H}}' = \frac{j\bar{k}_t}{\mu_o s}\frac{d\tilde{\Phi}}{d\xi_3} - \frac{k_t^2}{\mu_o s}\tilde{\Phi}\bar{a}_{\xi 3} \tag{9b}$$

in which $\tilde{\Phi}(\xi_3)$ satisfies

$$\frac{d^2\tilde{\Phi}}{d\xi_3^2} - [k_t^2 + \mu_o s(\sigma_t + s\varepsilon_t)]\tilde{\Phi} = 0 \tag{10}$$

and $k_t^2 = \bar{k}_t \cdot \bar{k}_t$. The parallel-polarized part of the field is derivable from a scalar function $\tilde{\Psi}(\xi_3)$ as

$$\tilde{\bar{E}}'' = \frac{-j\bar{k}_t}{\sigma_t + s\varepsilon_t}\frac{d\tilde{\Psi}}{d\xi_3} + \frac{k_t^2}{\sigma_\ell + s\varepsilon_\ell}\tilde{\Psi}\bar{a}_{\xi 3} \tag{11a}$$

---

†We assume that $\bar{\bar{\sigma}} + s\bar{\bar{\varepsilon}} = (\sigma_t + s\varepsilon_t)(\bar{a}_{\xi 1}\bar{a}_{\xi 1} + \bar{a}_{\xi 2}\bar{a}_{\xi 2}) + (\sigma_\ell + s\varepsilon_\ell)\bar{a}_{\xi 3}\bar{a}_{\xi 3}$.

$$\tilde{\bar{H}}'' = -j\bar{k}_t \times \bar{a}_{\xi 3}\tilde{\Psi} \tag{11b}$$

where $\tilde{\Psi}(\xi_3)$ satisfies

$$\frac{d^2\tilde{\Psi}}{d\xi_3^2} - [k_t^2 \left(\frac{\sigma_t + s\varepsilon_t}{\sigma_\ell + s\varepsilon_\ell}\right) + s\mu_o(\sigma_t + s\varepsilon_t)]\tilde{\Psi} = 0 \tag{12}$$

As is apparent, this formulation can be used for either the graphite composites (where $\sigma_\ell = 0$ and $s\varepsilon_t$ is ignored in comparison to σ_t) or the boron-epoxy composites (where $\sigma_\ell = \sigma_t = 0$).

Let us define the following quantities:

$$\kappa_3'^2 = k_t^2 + \mu_o s(\sigma_t + s\varepsilon_t) \tag{13a}$$

$$\kappa_3''^2 = k_t^2 \left(\frac{\sigma_t + s\varepsilon_t}{\sigma_\ell + s\varepsilon_\ell}\right) + s\mu_o(\sigma_t + s\varepsilon_t) \tag{13b}$$

Then it is easy to show that the tangential components of $\tilde{\bar{E}}$ and $\tilde{\bar{H}}$, denoted by subscript t, are given by

$$\tilde{\bar{E}}_t'(\xi_3) = -j\bar{k}_t \times \bar{a}_{\xi 3}(A' \cosh \kappa_3'\xi_3 + B' \sinh \kappa_3'\xi_3) \tag{14a}$$

$$\tilde{\bar{H}}_t'(\xi_3) = \frac{j\bar{k}_t}{\mu_o s}\kappa_3'(A' \sinh \kappa_3'\xi_3 + B' \cosh \kappa_3'\xi_3) \tag{14b}$$

$$\tilde{\bar{E}}_t''(\xi_3) = \frac{-j\bar{k}_t}{\sigma_t + s\varepsilon_t}\kappa_3''(A'' \sinh \kappa_3''\xi_3 + B'' \cosh \kappa_3''\xi_3) \tag{14c}$$

$$\tilde{\bar{H}}_t''(\xi_3) = -j\bar{k}_t \times \bar{a}_{\xi 3}(A'' \cosh \kappa_3''\xi_3 + B'' \sinh \kappa_3''\xi_3) \tag{14d}$$

in which $A^{','}$ and $B^{','}$ are constants.

We wish to find the relation between the fields at $\xi_3 = d$ and $\xi_3 = 0$. A straightforward analysis of eq. (14) yields

$$\begin{bmatrix} \tilde{\bar{E}}_t'(d) \\ \tilde{\bar{H}}_t'(d) \end{bmatrix} = \begin{bmatrix} C'\bar{\bar{I}} \cdot & \frac{\mu_o s}{\kappa_3'} S' \bar{a}_{\xi 3} \times \bar{\bar{I}} \cdot \\ \frac{-\kappa_3'}{\mu_o s} S'\bar{a}_{\xi 3} \times \bar{\bar{I}} \cdot & C'\bar{\bar{I}} \cdot \end{bmatrix} \begin{bmatrix} \tilde{\bar{E}}_t'(0) \\ \tilde{\bar{H}}_t'(0) \end{bmatrix} \tag{15a}$$

$$\begin{bmatrix} \tilde{\bar{E}}_t''(d) \\ \tilde{\bar{H}}_t''(d) \end{bmatrix} = \begin{bmatrix} C''\bar{\bar{I}} \cdot & \frac{\kappa_3'' S''}{(\sigma_t + s\varepsilon_t)} \bar{a}_{\xi 3} \times \bar{\bar{I}} \cdot \\ \frac{-(\sigma_t + s\varepsilon_t)}{\kappa_3''} S'' \bar{a}_{\xi 3} \times \bar{\bar{I}} \cdot & C''\bar{\bar{I}} \cdot \end{bmatrix} \begin{bmatrix} \tilde{\bar{E}}_t''(0) \\ \tilde{\bar{H}}_t''(0) \end{bmatrix} \tag{15b}$$

in which $C^{','} = \cosh \kappa_3^{','} d$, $S^{','} = \sinh \kappa_3^{','} d$, and $\bar{\bar{I}}$ denotes the idemfactor.

Now in order to account for the existence of boundaries between the shield material and the exterior media, we introduce the connection between fields on either side of a boundary which may contain a sheet admittance. It is assumed that such a sheet admittance is a scalar quantity for each polarization of the field; it relates the surface current density $\tilde{\bar{J}}_s$ at the sheet, which is located at $\xi_3 = \xi_{3s}$, to the tangential electric field there, which is assumed to be continuous through the sheet:

$$Y_s^{','} \tilde{\bar{E}}_t^{','}(\xi_{3s}) = \tilde{\bar{J}}_s^{','} \tag{16}$$

It is thus immediately apparent that at such a boundary,

$$\begin{bmatrix} \tilde{\bar{E}}_t^{','}(\xi_{3s}-) \\ \tilde{\bar{H}}_t^{','}(\xi_{3s}-) \end{bmatrix} = \begin{bmatrix} \bar{\bar{I}}\cdot & \bar{\bar{0}}\cdot \\ Y_s^{','}\bar{a}_{\xi 3}\times\bar{\bar{I}}\cdot & \bar{\bar{I}}\cdot \end{bmatrix} \begin{bmatrix} \tilde{\bar{E}}_t^{','}(\xi_{3s}+) \\ \tilde{\bar{H}}_t^{','}(\xi_{3s}+) \end{bmatrix} \tag{17}$$

$\bar{\bar{0}}$ denotes the null dyadic.

We now construct the connection between the fields in free space on either side of a composite laminate of thickness d, having a sheet admittance on the side $\xi_3 = 0$; the laminate occupies the region $0 \leq \xi_3 \leq d$. We readily obtain the following:

$$\begin{bmatrix} \tilde{\bar{E}}_t^{','}(0-) \\ \eta_o\, \tilde{\bar{H}}_t^{','}(0-) \end{bmatrix} = \begin{bmatrix} \bar{\bar{M}}_{11}^{','}\cdot & \bar{\bar{M}}_{12}^{','}\cdot \\ \bar{\bar{M}}_{21}^{','}\cdot & \bar{\bar{M}}_{22}^{','}\cdot \end{bmatrix} \begin{bmatrix} \tilde{\bar{E}}_t^{','}(d+) \\ \eta_o\, \tilde{\bar{H}}_t^{','}(d+) \end{bmatrix} \tag{18}$$

where

$$\bar{\bar{M}}_{11}' = \cosh \kappa_3' d\ \bar{\bar{I}} \tag{19a}$$

$$\bar{\bar{M}}_{12}' = \frac{-s}{c\kappa_3'} \sinh \kappa_3' d\ \bar{a}_{\xi 3} \times \bar{\bar{I}} \tag{19b}$$

$$\bar{\bar{M}}_{21}' = (\eta_o Y_s' \cosh \kappa_3' d + \frac{c\kappa_3'}{s} \sinh \kappa_3' d)\bar{a}_{\xi 3} \times \bar{\bar{I}} \tag{19c}$$

$$\bar{\bar{M}}_{22}' = (\eta_o Y_s' \frac{s}{c\kappa_3'} \sinh \kappa_3' d + \cosh \kappa_3' d)\bar{\bar{I}} \tag{19d}$$

$$\overline{\overline{M}}''_{11} = \cosh \kappa''_3 d \; \overline{\overline{I}} \tag{19e}$$

$$\overline{\overline{M}}''_{12} = \frac{-\kappa''_3}{\eta_o(\sigma_t + s\epsilon_t)} \sinh \kappa''_3 d \; \bar{a}_{\xi 3} \times \overline{\overline{I}} \tag{19f}$$

$$\overline{\overline{M}}''_{21} = (\eta_o Y''_s \cosh \kappa''_3 d + \eta_o \frac{\sigma_t + s\epsilon_t}{\kappa''_3} \sinh \kappa''_3 d)\bar{a}_{\xi 3} \times \overline{\overline{I}} \tag{19g}$$

$$\overline{\overline{M}}''_{22} = (\eta_o Y''_s \frac{\kappa''_3}{\eta_o(\sigma_t + s\epsilon_t)} \sinh \kappa''_3 d + \cosh \kappa''_3 d)\overline{\overline{I}} \tag{19h}$$

$c = 1/\sqrt{\mu_o \epsilon_o}$, the speed of light in vacuum, and $\eta_o = \sqrt{\mu_o/\epsilon_o}$, the characteristic impedance of vacuum. Equations (18) and (19) represent the field connection relation which we shall use in the analysis of the two reflection and transmission problems to which we have earlier alluded. The factors η_o have been inserted to make the matrix elements all dimensionless.

A. Determination of Constitutive Parameters

We consider first the evaluation of $\sigma_{\ell 1}$ for the graphite composite lamina (cf. Fig. (4)). We assume that the fiber radius r_f is not large in comparison with the skin depth at frequencies of interest, so that the fiber is completely penetrated by the component of electric field parallel to the fiber axis. We further assume that the neighboring fibers do not disturb the current density distribution in a given fiber, which is therefore taken to be uniform. Denoting by E_{1f} the axial electric field component at a fiber, the fiber current I_f is given by

$$I_f = \pi r_f^2 \, \sigma_g E_{1f} \tag{20}$$

in which σ_g denotes the graphite fiber conductivity. The "incident" field at the fibers (the primary field) is $E_{10}\bar{a}_{\xi 1}$.

The total field E_{1t} due to the fiber array is easily shown to be

$$E_{1t} = \frac{-s\mu_o}{2\pi} I_f \sum_{n=-\infty}^{\infty} K_o \left(s\sqrt{\mu_o \epsilon_m} \sqrt{(\xi_2 - na)^2 + \xi_3^2}\right) \tag{21}$$

and the field E_{1f}, due to the field E_{10} and the fields of the neighboring fibers, is thus

$$E_{1f} = E_{10} - \frac{s\mu_o}{\pi} I_f \sum_{n=1}^{\infty} K_o(sna\sqrt{\mu_o\varepsilon_m}) \tag{22}$$

The fiber current I_f expressed in terms of the field E_{10} is

$$I_f = \pi r_f^2 \sigma_g E_{10}\left[1 + \frac{\eta_m \sigma_g d_\ell}{2}\left(\frac{\pi r_f^2}{a d_\ell}\right) \frac{2}{\pi} sa\sqrt{\mu_o\varepsilon_m} \sum_{n=1}^{\infty} K_o(san\sqrt{\mu_o\varepsilon_m})\right]^{-1} \tag{23}$$

where $\eta_m = \sqrt{\mu_o/\varepsilon_m}$ is the characteristic impedance of the epoxy matrix. Now $|sa\sqrt{\mu_o\varepsilon_m}| << 1$ at all frequencies of interest, and

$$\lim_{x\to 0} x \sum_{n=1}^{\infty} K_o(nx) = \frac{\pi}{2} \tag{24}$$

as is easy to show. Hence

$$I_f \simeq \pi r_f^2 \sigma_g E_{10}\left[1 + \frac{\eta_m \sigma_g d_\ell}{2}\left(\frac{\pi r_f^2}{a d_\ell}\right)\right]^{-1} \tag{25}$$

Now the average (over coordinate ξ_2) electric field E_1 at $|\xi_3| = d_\ell/2$ is, if $|s\sqrt{\mu_o\varepsilon_m}\, d_\ell/2| << 1$,

$$E_{1a} = E_{10} - \frac{\eta_m}{2a} I_f \tag{26}$$

so defining $\sigma_{\ell 1}$ through

$$\sigma_{\ell 1} E_{1a} = \frac{I_f}{a d_\ell} \tag{27}$$

we immediately obtain the expected result

$$\sigma_{\ell 1} = \sigma_g\left(\frac{\pi r_f^2}{a d_\ell}\right) \tag{28}$$

Let us denote the volume fraction occupied by the fibers by $q \equiv \pi r_f^2/a d_\ell$; then $\sigma_{\ell 1} = q\sigma_g$.

We determine the permittivity $\varepsilon_{\ell 1}$ by a similar procedure, except that we begin by assuming that the fiber current is given by

$$I_f = \pi r_f^2 s(\varepsilon_f - \varepsilon_m)E_{1f} \tag{29}$$

for the boron-epoxy composite, in which ε_f denotes the permittivity of the boron fibers. The result is

$$\varepsilon_{\ell 1} = \varepsilon_f q + \varepsilon_m(1-q)$$
$$= q(\varepsilon_f - \varepsilon_m) + \varepsilon_m \qquad (30)$$

The determination of the permittivities $\varepsilon_{\ell 2}$ and $\varepsilon_{\ell 3}$ may be done using an electrostatic model. In each case a uniform electric field $E_o\bar{a}_{\xi i}$ (i = 2,3) is applied to the one-dimensional fiber array and the resulting polarization is determined.

Consider first the case where the uniform electric field is $E_o\bar{a}_{\xi 2}$. Then the potential outside the fibers is

$$V(\xi_2,\xi_3) = -E_o\xi_2 + \frac{p}{2\pi\varepsilon_m}\sum_{n=-\infty}^{\infty}\frac{\xi_2 - na}{(\xi_2-na)^2 + \xi_3^2} \qquad (31)$$

in which p denotes the line dipole moment of a single cylindrical fiber. The field $E_{\xi 20}$ at $\xi_2 = \xi_3 = 0$ due to the applied field and the presence of all the fibers except that at $\xi_2 = 0$ is

$$E_{\xi 20} = E_o + \frac{p}{\pi\varepsilon_m a^2}\sum_{n=1}^{\infty}\frac{1}{n^2}$$
$$= E_o + \frac{p}{\pi\varepsilon_m a^2}\left(\frac{\pi^2}{6}\right) \qquad (32)$$

from which it is evident that if $p = \alpha_e\varepsilon_m E_{\xi 20}$, where α_e denotes the polarizability of the fiber,

$$p = \frac{\alpha_e\varepsilon_m}{1 - \alpha_e\pi/6a^2}E_o \qquad (33)$$

The induced dipole moment per unit volume in the lamina is simply p/ad_ℓ, so that in the lamina, on the average,

$$D_{\xi 2} = \varepsilon_m E_o[1 + \frac{\alpha_e/ad_\ell}{1 - \alpha_e\pi/6a^2}] \equiv \varepsilon_{\ell 2}E_o \qquad (34)$$

Now α_e is given by

$$\alpha_e = 2\pi r_f^2\left(\frac{\varepsilon_f - \varepsilon_m}{\varepsilon_f + \varepsilon_m}\right) \qquad (35)$$

for boron-epoxy composite laminae and by

$$\alpha_e = 2\pi r_f^2 \qquad (36)$$

for graphite composite laminae. Thus we obtain

$$\varepsilon_{\ell 2} = \varepsilon_m \frac{1 + 2qf(1 - \pi d_\ell/6a)}{1 - 2qf(\pi d_\ell/6a)} \tag{37}$$

in which q is the volume fraction occupied by the fibers and

$$f = \begin{cases} 1 & \text{, for graphite composites} \\ \dfrac{\varepsilon_f - \varepsilon_m}{\varepsilon_f + \varepsilon_m} & \text{, for boron-epoxy composites} \end{cases} \tag{38}$$

A similar analysis carried out for an applied field $E_o\bar{a}_{\xi 3}$ yields the result that

$$\varepsilon_{\ell 3} = \varepsilon_m \frac{1 + 2qf(1 + \pi d_\ell/6a)}{1 + 2qf\pi d_\ell/6a} \tag{39}$$

It is not our purpose here to conduct a detailed exploration of the behavior of the constitutive parameters as functions of the variables q, $\varepsilon_f/\varepsilon_m$, and d_ℓ/a. Rather we shall focus attention on a typical case, in order to obtain estimates of the parameters which will be used in our later analysis. We shall consider as typical the values $q = 1/3$, $d_\ell/a = \pi/3 \simeq 1$. We thus find that for graphite laminate panels,

$$\sigma_t \equiv \frac{1}{2}\,\sigma_{\ell 1} = \frac{1}{6}\,\sigma_g \tag{40a}$$

$$\varepsilon_\ell \equiv \varepsilon_{\ell 3} = \frac{3}{2}\,\varepsilon_m \tag{40b}$$

and for boron-epoxy panels,

$$\varepsilon_t \equiv \frac{1}{2}\,(\varepsilon_{\ell 1} + \varepsilon_{\ell 2}) = \frac{1}{6}\,(\varepsilon_f + 5\varepsilon_m) \tag{41a}$$

$$\varepsilon_\ell \equiv \varepsilon_{\ell 3} = \varepsilon_m \left(\frac{3\varepsilon_f}{\varepsilon_m + 2\varepsilon_f}\right) \tag{41b}$$

We shall now apply these results to the remainder of the boundary-value problems mentioned earlier, beginning with the treatment of the graphite composite skin panel.

B. Electromagnetic Plane Wave Penetration of a Graphite Composite Skin Panel

The geometry of the problem we shall consider is shown in Fig. (5). A graphite composite laminate of infinite transverse extent fills the region

$0 \leq z \leq d$. An electromagnetic plane wave impinges on the laminate from the region $z < 0$. The problem is to determine the reflected and transmitted fields. It will be recalled that the graphite composite laminate has been modelled as an anisotropically conductive slab. Specializing the various quantities in eqs. (13) to this case, we obtain

$$\kappa_3'^2 = s\mu_o\sigma_t = s\tau_d'/d^2 \tag{42a}$$

$$\kappa_3''^2 = s\mu_o\sigma_t\left(1 - \frac{\sin^2\theta}{\epsilon_{\ell r}}\right) = s\tau_d''/d^2 \tag{42b}$$

where τ_d' and τ_d'' are the shield diffusion time constants and in which $\epsilon_{\ell r} = \epsilon_\ell/\epsilon_o$ and θ denotes the angle of incidence. It is immediately apparent that insofar as the perpendicular-polarized field is concerned, the graphite laminate behaves as an isotropic conducting slab of conductivity σ_t. For the parallel-polarized field, the shield diffusion time τ_d'' depends upon the angle of incidence and the "longitudinal" permittivity ϵ_ℓ. We obtain for the matrix elements $\bar{\bar{M}}_{ij}',''$

$$\bar{\bar{M}}_{11}',''= \bar{\bar{I}} \cosh\sqrt{s\tau_d',''} \tag{43a}$$

$$\bar{\bar{M}}_{12}','' = -\frac{sd}{c}\frac{\sinh\sqrt{s\tau_d',''}}{\sqrt{s\tau_d',''}}\,\bar{a}_z \times \bar{\bar{I}} \tag{43b}$$

$$\bar{\bar{M}}_{21}','' = \eta_o\sigma_t d\,\frac{\sinh\sqrt{s\tau_d',''}}{\sqrt{s\tau_d',''}}\,\bar{a}_z \times \bar{\bar{I}} \tag{43c}$$

$$\bar{\bar{M}}_{22}','' = \bar{\bar{I}} \cosh\sqrt{s\tau_d',''} \tag{43d}$$

These elements completely characterize the graphite composite panel for frequencies at which the transverse conduction currents dominate the displacement currents. We shall now show that the elements $\bar{\bar{M}}_{12}',''$ can be neglected entirely with respect to $\bar{\bar{M}}_{21}',''$ insofar as the reflected and transmitted fields are concerned.

Consider first the reflection and transmission of a perpendicular-polarized plane wave by the panel. We have incident, reflected, and transmitted fields given as follows:

$$\bar{E}'_{inc} = E'_o \bar{a}_y \; e^{-s/c(x \sin\theta + z \cos\theta)} \tag{44a}$$

$$\eta_o \; \bar{H}'_{inc} = E'_o(\bar{a}_z \sin\theta - \bar{a}_x \cos\theta) e^{-s/c(x \sin\theta + z \cos\theta)} \tag{44b}$$

$$\bar{E}'_{ref} = R' E'_o \bar{a}_y \; e^{-s/c(x \sin\theta - z \cos\theta)} \tag{44c}$$

$$\eta_o \; \bar{H}'_{ref} = R' E'_o(\bar{a}_z \sin\theta + \bar{a}_x \cos\theta) e^{-s/c(x \sin\theta - z \cos\theta)} \tag{44d}$$

$$\bar{E}'_{trans} = T' E'_o \bar{a}_y \; e^{-s/c[x \sin\theta + (z-d)\cos\theta]} \tag{44e}$$

$$\eta_o \; \bar{E}'_{trans} = T' E'_o(\bar{a}_z \sin\theta - \bar{a}_x \cos\theta) e^{-s/c[x \sin\theta + (z-d)\cos\theta]} \tag{44f}$$

Therefore we immediately obtain

$$\tilde{\bar{E}}'_t(0) = (1+R')E'_o \bar{a}_y \tag{45a}$$

$$\eta_o \; \tilde{\bar{H}}'_t(0) = -\cos\theta(1-R')E'_o \bar{a}_x \tag{45b}$$

$$\tilde{\bar{E}}'_t(d) = T' E'_o \bar{a}_y \tag{45c}$$

$$\eta_o \; \tilde{\bar{H}}'_t(d) = -\cos\theta \; T' E'_o \bar{a}_x \tag{45d}$$

Connecting these fields across the graphite composite panel using eqs. (18) and (21) yields a pair of equations for the reflection and transmission coefficients R' and T':

$$\begin{bmatrix} 1 & -\cosh\sqrt{s\tau'_d} - \frac{sd}{c}\cos\theta \, \frac{\sinh\sqrt{s\tau'_d}}{\sqrt{s\tau'_d}} \\ \cos\theta & \cos\theta \, \cosh\sqrt{s\tau'_d} + \eta_o \sigma_t d \, \frac{\sinh\sqrt{s\tau'_d}}{\sqrt{s\tau'_d}} \end{bmatrix} \begin{bmatrix} R' \\ T' \end{bmatrix} = \begin{bmatrix} -1 \\ \cos\theta \end{bmatrix} \tag{46}$$

Solving for R' and T' yields

$$R' = \frac{1}{D'} \left(\frac{sd}{c} \cos^2\theta - \eta_o \sigma_t d\right) \frac{\sinh\sqrt{s\tau'_d}}{\sqrt{s\tau'_d}} \tag{47a}$$

$$T' = \frac{1}{D'} \; (2\cos\theta) \tag{47b}$$

with

$$D' = 2\cos\theta \cosh \sqrt{s\tau'_d} + (\eta_o \sigma_t d + \frac{sd}{c} \cos^2\theta) \frac{\sinh \sqrt{s\tau'_d}}{\sqrt{s\tau'_d}} \qquad (48)$$

Now neglecting $sd/c \cos^2\theta$ with respect to $\eta_o \sigma_t d$ is justified for all angles θ, in the frequency range where graphite can be considered a good conductor. Thus

$$R' \approx \frac{-\eta_o \sigma_t d}{2} \sec\theta \frac{\sinh \sqrt{s\tau'_d}}{\sqrt{s\tau'_d}} T' \qquad (49a)$$

$$T' \approx [\cosh \sqrt{s\tau'_d} + \frac{\eta_o \sigma_t d}{2} \sec\theta \frac{\sinh \sqrt{s\tau'_d}}{\sqrt{s\tau'_d}}]^{-1} \qquad (49b)$$

It is immediately clear that the "effective" values of the elements $\overline{\overline{M}}'_{ij}$ are

$$\overline{\overline{M}}'_{11} = \overline{\overline{M}}'_{22} = \cosh \sqrt{s\tau'_d}\ \overline{\overline{I}} \qquad (50a)$$

$$\overline{\overline{M}}'_{12} = \overline{\overline{0}} \qquad (50b)$$

$$\overline{\overline{M}}'_{21} = \eta_o \sigma_t d \frac{\sinh \sqrt{s\tau'_d}}{\sqrt{s\tau'_d}} \bar{a}_z \times \overline{\overline{I}} \qquad (50c)$$

in that these values for $\overline{\overline{M}}'_{ij}$ yield eqs. (49) directly.

It is interesting to express the relation (18) for perpendicular polarization as follows, using eqs. (50):

$$\begin{bmatrix} \tilde{\bar{E}}'_t(0-) \\ \eta_o \tilde{\bar{H}}'_t(0-) \end{bmatrix} = \cosh\sqrt{s\tau'_d} \begin{bmatrix} \overline{\overline{I}} \cdot & \overline{\overline{0}} \cdot \\ \eta_o Y'_{s,eq}\ \bar{a}_z \times \overline{\overline{I}} \cdot & \overline{\overline{I}} \cdot \end{bmatrix} \begin{bmatrix} \tilde{\bar{E}}'_t(d+) \\ \eta_o \tilde{\bar{H}}'_t(d+) \end{bmatrix} \qquad (51)$$

in which

$$\eta_o Y'_{s,eq} = \eta_o \sigma_t d \frac{\tanh \sqrt{s\tau'_d}}{\sqrt{s\tau'_d}} \qquad (52)$$

Comparing eq. (51) with eq. (17), we see that the graphite composite pane can be modeled as an equivalent sheet admittance, even if $|\sqrt{s\tau_d'}|$ is not small in comparison to unity, if the "extra" factor $\cosh \sqrt{s\tau_d'}$ is extracte as shown in eq. (51). Naturally if $|\sqrt{s\tau_d'}| << 1$, we obtain the expected result

$$\eta_o Y_{s,eq}' \Big|_{s\tau_d' \to 0} = \eta_o \sigma_t d \tag{53}$$

Now consider the parallel-polarized fields. The incident, reflected, and transmitted fields are given by

$$\bar{E}''_{inc} = E''_o(\bar{a}_x \cos\theta - \bar{a}_z \sin\theta)e^{-s/c(x \sin\theta + z \cos\theta)} \tag{54a}$$

$$\eta_o \, \bar{\bar{H}}''_{inc} = E''_o \bar{a}_y \, e^{-s/c(x \sin\theta + z \cos\theta)} \tag{54b}$$

$$\bar{E}''_{ref} = -R''E''_o(\bar{a}_x \cos\theta + \bar{a}_z \sin\theta)e^{-s/c(x \sin\theta - z \cos\theta)} \tag{54c}$$

$$\eta_o \, \bar{H}''_{ref} = R''E''_o \bar{a}_y e^{-s/c(x \sin\theta - z \cos\theta)} \tag{54d}$$

$$\bar{E}''_{trans} = T''E''_o(\bar{a}_x \cos\theta - \bar{a}_z \sin\theta)e^{-s/c[x \sin\theta + (z-d)\cos\theta]} \tag{54e}$$

$$\eta_o \, \bar{H}''_{trans} = T''E''_o \bar{a}_y \, e^{-s/c \, [x \sin\theta + (z-d)\cos\theta]} \tag{54f}$$

and the tangential field components at the boundaries z=0 and z=d are

$$\bar{\bar{E}}''_t(0) = \cos\theta(1-R'')E''_o \, \bar{a}_x \tag{55a}$$

$$\eta_o \, \bar{\bar{H}}''_t(0) = (1+R'')E''_o \, \bar{a}_y \tag{55b}$$

$$\bar{\bar{E}}''_t(d) = \cos\theta \; T''E''_o \, \bar{a}_x \tag{55c}$$

$$\eta_o \, \bar{\bar{H}}''_t(d) = T''E''_o \, \bar{a}_y \tag{55d}$$

Now connecting these field components across the graphite composite panel using eqs. (18) and (21) yields two relations between the reflection and transmission coefficients R" and T" as follows:

$$\begin{bmatrix} \cos\theta & \cos\theta \cosh \sqrt{s\tau_d''} + \dfrac{sd}{c} \dfrac{\sinh \sqrt{s\tau_d''}}{\sqrt{s\tau_d''}} \\ & \\ -1 & \cosh \sqrt{s\tau_d''} + \eta_o \sigma_t d \cos\theta \dfrac{\sinh \sqrt{s\tau_d''}}{\sqrt{s\tau_d''}} \end{bmatrix} \begin{bmatrix} R'' \\ \\ T'' \end{bmatrix} = \begin{bmatrix} \cos\theta \\ \\ 1 \end{bmatrix} \tag{56}$$

from which we obtain

$$R'' = \frac{1}{D''} (\eta_o \sigma_t d \cos^2\theta - \frac{sd}{c}) \frac{\sinh\sqrt{s\tau''_d}}{\sqrt{s\tau''_d}} \tag{57a}$$

$$T'' = \frac{1}{D''} (2\cos\theta) \tag{57b}$$

where

$$D'' = 2\cos\theta \cosh \sqrt{s\tau''_d} + (\eta_o \sigma_t d \cos^2\theta + \frac{sd}{c}) \frac{\sinh \sqrt{s\tau''_d}}{\sqrt{s\tau''_d}} \tag{58}$$

It is apparent that for frequencies at which the graphite composite can be considered a good conductor and for angles of incidence not too close to 90°, sd/c can be neglected in comparison to $\eta_o \sigma_t d \cos^2\theta$, so that

$$R'' \simeq \frac{1}{2} \eta_o \sigma_t d \cos\theta \frac{\sinh \sqrt{s\tau''_d}}{\sqrt{s\tau''_d}} T'' \tag{59a}$$

$$T'' \simeq [\cosh \sqrt{s\tau''_d} + \frac{\eta_o \sigma_t d}{2} \cos\theta \frac{\sinh \sqrt{s\tau''_d}}{\sqrt{s\tau''_d}}]^{-1} \tag{59b}$$

The "effective" values of the elements $\overline{\overline{M}}''_{ij}$ under these conditions are therefore

$$\overline{\overline{M}}''_{11} = \overline{\overline{M}}''_{22} = \cosh \sqrt{s\tau''_d}\ \overline{\overline{I}} \tag{60a}$$

$$\overline{\overline{M}}''_{12} = \overline{\overline{0}} \tag{60b}$$

$$\overline{\overline{M}}''_{21} = \eta_o \sigma_t d \frac{\sinh \sqrt{s\tau''_d}}{\sqrt{s\tau''_d}} \bar{a}_z \times \overline{\overline{I}} \tag{60c}$$

Furthermore, a "semi-equivalent" sheet admittance $Y''_{s,eq}$ can be defined exactly as in eqs. (51) and (52); we merely replace the single primes (') with double primes (") in those expressions.

C. Electromagnetic Plane Wave Penetration of a Screened Boron-Epoxy Skin Panel

The geometry of the problem we shall consider is shown in Fig. (6). A boron-epoxy composite laminate of infinite transverse extent fills the region $0 \le z \le d$. A wire-mesh screen is in the surface z=0. The screen is described by a sheet admittance $\overline{\overline{Y}}_s$ which diagonalizes for perpendicular or parallel-polarized fields; the eigenvalues for these cases are Y_s' and Y_s'' respectively. A plane electromagnetic wave impinges on the laminate from the region z<0. The object of the analysis is to determine the reflected and the transmitted fields and to determine the equivalent admittances $Y_{se}^{','\,''}$.

For the boron-epoxy composite, κ_3' and κ_3'' are given by

$$\kappa_3'^2 = k_t^2 + s^2\mu_o\varepsilon_t \tag{61a}$$

$$\kappa_3''^2 = k_t^2 \frac{\varepsilon_t}{\varepsilon_\ell} + s^2\mu_o\varepsilon_t \tag{61b}$$

When the incident wave is perpendicular-polarized, we obtain the following expressions for the reflection and transmission coefficients R' and T', using a procedure similar to that carried out in the previous section:

$$R' = -\frac{1}{D'}\left[\eta_o Y_s'\left(\cosh \kappa_3' d + \frac{sd}{c}\cos\theta\,\frac{\sinh \kappa_3' d}{\kappa_3' d}\right)\right.$$
$$\left. + \left(-\frac{sd}{c}\cos^2\theta + \frac{c}{sd}\kappa_3'^2 d^2\right)\frac{\sinh \kappa_3' d}{\kappa_3' d}\right] \tag{62a}$$

$$T' = \frac{2\cos\theta}{D'} \tag{62b}$$

in which

$$D' = 2\cos\theta\,\cosh \kappa_3' d + \left(\frac{sd}{c}\cos^2\theta + \frac{c\kappa_3'^2 d^2}{sd}\right)\frac{\sinh \kappa_3' d}{\kappa_3' d}$$
$$+ \eta_o Y_s'\left(\cosh \kappa_3' d + \frac{sd}{c}\cos\theta\,\frac{\sinh \kappa_3' d}{\kappa_3' d}\right) \tag{63}$$

These results may be greatly simplified by noting that over the frequency range of interest the boron-epoxy laminate is electrically thin, so that $|\kappa_3' d| \ll 1$. We thus obtain

$$R' \approx \frac{-\eta_o\ Y'_{se}}{2\cos\theta + \eta_o\ Y'_{se}} \tag{64a}$$

$$T' \approx \frac{2\cos\theta}{2\cos\theta + \eta_o\ Y'_{se}}\ e^{-sd/c\ \cos\theta} \tag{64b}$$

in which the factor $\exp(-sd/c\ \cos\theta)$ is included in T' to refer the phase of the transmitted field to $z=0$, and

$$\eta_o\ Y'_{se} = \eta_o\ Y'_s + \frac{sd}{c}\ (\epsilon_{tr} - 1) \tag{65}$$

is the normalized equivalent admittance of the wire screen and the boron-epoxy composite panel, for perpendicular polarization. $\epsilon_{tr} = \epsilon_t/\epsilon_o$. In a practical configuration, the normalized screen admittance $\eta_o\ Y'_s$ will greatly exceed that of the laminate panel $sd/c\ (\epsilon_{tr} - 1)$, which may therefore be neglected.

When the incident wave is polarized parallel to the plane of incidence, the reflection and transmission coefficients R'' and T'' are given by

$$R'' = \frac{1}{D''}\left\{\eta_o Y''_s\ [1 + \sec\theta\ \frac{sd}{c}\left(1 - \frac{\sin^2\theta}{\epsilon_{\ell r}}\right)] + \epsilon_{tr}\ \frac{sd}{c}\right\} \tag{66a}$$

$$T'' = \frac{2\sec\theta}{D''} \tag{66b}$$

where

$$D'' = \eta_o Y''_s[1 + \sec\theta\ \frac{sd}{c}\left(1 - \frac{\sin^2\theta}{\epsilon_{\ell r}}\right)] + \frac{sd}{c}\ [\epsilon_{tr} + \sec^2\theta\left(1 - \frac{\sin^2\theta}{\epsilon_{\ell r}}\right)] + 2\sec\theta \tag{67}$$

in which we have assumed that $|\kappa''_3 d| << 1$. It is not possible to construct an equivalent sheet admittance Y''_{se} for this polarization except under special circumstances. However, if θ is not too near 90°, we may write

$$R'' \approx \frac{\eta_o Y''_{se}}{2\sec\theta + \eta_o Y''_{se}} \tag{68a}$$

$$T'' \approx \frac{2\sec\theta}{2\sec\theta + \eta_o Y''_{se}} \tag{68b}$$

in which

$$\eta_o Y''_{se} = \eta_o Y''_s + \frac{sd}{c}\ \epsilon_{tr} \tag{69}$$

It is assumed that $|\sec\theta \; sd/c \; (1-\sin^2\theta/\varepsilon_{\ell r})| \ll 1$ and $\sec^2\theta(1-\sin^2\theta/\varepsilon_{\ell r}) \ll \varepsilon_{tr}$. The first assumption will be valid in the frequency range of interest if θ is not too near 90°; the second assumption is questionable. However, it will happen that $|\eta_o Y_s''|$ will be large in comparison to $|sd\varepsilon_{tr}/c|$, so a good approximation to Y_{se}'' is simply Y_s''. This must not be construed, however, as implying that the boron-epoxy laminate has no influence; as we shall see in the next section, Y_s'' depends on the dielectric properties of the composite slab on which the wire mesh screen is placed.

We conclude this section by noting that the screened boron-epoxy composite panel can be modeled (at least under most conditions) by an equivalent sheet admittance Y_{se}' or Y_{se}''; also, $Y_{se}^{','',} \approx Y_s^{','',}$. Thus the connection relation for the electromagnetic field across the panel is roughly that given in eq. (18), with

$$\overline{\overline{M}}_{11}^{','',} = \overline{\overline{I}} = \overline{\overline{M}}_{22}^{','',}$$

$$\overline{\overline{M}}_{12}^{','',} = \overline{\overline{0}} \tag{70}$$

$$\overline{\overline{M}}_{21}^{','',} = \eta_o Y_s^{','',} \; \bar{a}_{\xi 3} \times \overline{\overline{I}}$$

The sheet admittances Y_s' and Y_s' are determined in the next section.

D. Effective Sheet Admittance of a Wire Mesh Screen in a Dielectric Interface

We consider the fine wire mesh screen shown in Fig. (3) and discussed in Section II,C. We neglect the finite thickness of the laminate for reasons already discussed and consider it to be infinitely thick. The screen resides, therefore, in the interface between two dielectric half-spaces. The half-space $z<0$ is free space and the half-space $z>0$ is uniaxially anisotropic, representing the composite laminate.

We express the x-directed currents in the wires at $y=qa_s$ ($q = 0, \pm 1, \pm 2, \ldots$) and the y-directed currents in the wires at $x = pa_s$ ($p = 0, \pm 1, \pm 2, \ldots$) as follows:

$$I_x(x,y=qa_s) = e^{-\kappa_{xo}x - \kappa_{yo}qa_s}\,[I_{xo} + \Delta f(x) + s_x g(x)] \tag{71a}$$

$$I_y(x=pa_s,y) = e^{-\kappa_{xo}pa_s - \kappa_{yo}y}\,[I_{yo} - \Delta f(y) - s_y g(y)] \tag{71b}$$

in which I_{xo}, I_{yo}, Δ, s_x, and s_y are to be determined,

$$\kappa_{xo} = \frac{s}{c}\sin\theta\,\cos\phi \tag{72a}$$

$$\kappa_{yo} = \frac{s}{c}\sin\theta\,\sin\phi \tag{72b}$$

and f(x) and g(x) are given by†

$$f(x) = \frac{-1}{2\pi j}\sum_{n=-\infty}^{\infty}{}' \frac{1}{n}\, e^{-2j\pi nx/a_s} \tag{73a}$$

$$g(x) = \frac{-a_s}{(2\pi)^2}\sum_{n=-\infty}^{\infty}{}' \frac{1}{n^2}\, e^{-2\pi jnx/a_s} \tag{73b}$$

f(x) is a sawtooth function of period a_s with unit jump discontinuities at $x = 0, \pm a_s, \ldots$, and g(x) is a function with unit slope discontinuities at these points. Both functions have zero average value. It will be noted that the expressions given in eq. (71) guarantee that Kirchhoff's current law is satisfied at the junctions.

We now impose further conditions on the currents. First, the linear charge densities on the "x-wires" and the "y-wires" are made to be continuous through the junctions. This condition readily yields the relations

$$s_x = \kappa_{xo}\Delta \tag{74a}$$

$$s_y = \kappa_{yo}\Delta \tag{74b}$$

Next, the charge densities on the x-wires and the y-wires are forced to be equal at the junctions (i.e., there is no potential difference across any junction -- the wires are bonded there). This condition yields

$$\Delta = a_s(\kappa_{yo}I_{yo} - \kappa_{xo}I_{xo})\left[2 + \frac{a_s^2}{12}(\kappa_{xo}^2 + \kappa_{yo}^2)\right]^{-1} \tag{75}$$

so that, if quantities of order $(sa_s/c)^2$ and higher are neglected,

†The primes on the summation signs in eq. (73) indicate that the n=0 term is omitted.

$$I_x(x) \simeq e^{-\kappa_{xo}x - \kappa_{yo}qa_s} \left[I_{xo} + \frac{a_s}{2} f(x)(\kappa_{yo}I_{yo} - \kappa_{xo}I_{xo})\right] \qquad (76a)$$

$$I_y(y) \simeq e^{-\kappa_{xo}pa - \kappa_{yo}a_s} \left[I_{yo} - \frac{a_s}{2} f(x)(\kappa_{yo}I_{yo} - \kappa_{xo}I_{xo})\right] \qquad (76b)$$

The surface current density $\bar{J}_s$ associated with these currents in the z=0 plane is

$$\bar{J}_s = \sum_{m=-\infty}^{\infty} \sum_{n=-\infty}^{\infty} e^{-jk_{xm}x - jk_{yn}y} (\bar{a}_x J_{sxm} + \bar{a}_y J_{syn}) \qquad (77)$$

in which

$$k_{xm} = -j\kappa_{xo} + \frac{2m\pi}{a_s} \qquad (78a)$$

$$k_{yn} = -j\kappa_{yo} + \frac{2n\pi}{a_s} \qquad (78b)$$

$$J_{sxm} = \frac{1}{a_s} I_{xo}\delta_{mo} - \frac{1}{4\pi jm} (\kappa_{yo}I_{yo} - \kappa_{xo}I_{xo})(1-\delta_{mo}) \qquad (78c)$$

$$J_{syn} = \frac{1}{a_s} I_{yo}\delta_{no} + \frac{1}{4\pi jn} (\kappa_{yo}I_{yo} - \kappa_{xo}I_{xo})(1-\delta_{no}) \qquad (78d)$$

and δ_{no} denotes the Kronecker delta-function. The electromagnetic field whose source is $\bar{J}_s$ is given by

$$\begin{bmatrix} \bar{E} \\ \bar{H} \end{bmatrix} = \sum_{m=-\infty}^{\infty} \sum_{n=-\infty}^{\infty} \begin{bmatrix} \tilde{\bar{E}}_{mn} \\ \tilde{\bar{H}}_{mn} \end{bmatrix} e^{-jk_{xm}x - jk_{yn}y} \qquad (79)$$

with

$$\tilde{\bar{E}}_{mn} = -j\bar{k}_{tmn} \times \bar{a}_z \tilde{\bar{\Phi}}_{mn} - \frac{j\bar{k}_{tmn}}{s\varepsilon_o\varepsilon_{tr}} \frac{d\tilde{\Psi}_{mn}}{dz} + \frac{k_{tmn}^2}{s\varepsilon_o\varepsilon_{\ell r}} \tilde{\Psi}_{mn}\bar{a}_z \,^{\dagger} \qquad (80a)$$

$$\tilde{\bar{H}}_{mn} = -j\bar{k}_{tmn} \times \bar{a}_z \tilde{\Psi}_{mn} + \frac{j\bar{k}_{tmn}}{s\mu_o} \frac{d\tilde{\Phi}_{mn}}{dz} - \frac{k_{tmn}^2}{s\mu_o} \tilde{\Phi}_{mn}\bar{a}_z \qquad (80b)$$

in which $\bar{k}_{tmn} = k_{xm}\bar{a}_x + k_{yn}\bar{a}_y$ and $k_{tmn}^2 = k_{xm}^2 + k_{yn}^2$. $\tilde{\Phi}_{mn}$ and $\tilde{\Psi}_{mn}$ satisfy the equations

$$\frac{d^2\tilde{\Phi}_{mn}}{dz^2} - \Gamma_{mn}^2 \tilde{\Phi}_{mn} = 0 \qquad (81a)$$

---

† For z<0, replace ε_{tr} and $\varepsilon_{\ell r}$ by 1.

$$\frac{d^2\tilde{\Psi}_{mn}}{dz^2} - \Lambda_{mn}^2 \tilde{\Psi}_{mn} = 0 \tag{81b}$$

where

$$\Lambda_{mn}^2 = \Gamma_{mn}^2 = \Gamma_{mno}^2 = k_{xm}^2 + k_{yn}^2 + \frac{s^2}{c^2} \qquad (z < 0) \tag{82a}$$

$$\Gamma_{mn}^2 = \Gamma_{mnd}^2 = k_{xm}^2 + k_{yn}^2 + \frac{s^2}{c^2}\,\varepsilon_{tr} \qquad (z > 0) \tag{82b}$$

$$\Lambda_{mn}^2 = \Lambda_{mnd}^2 = (k_{xm}^2 + k_{yn}^2)\,\frac{\varepsilon_{tr}}{\varepsilon_{\ell r}} + \frac{s^2}{c^2}\,\varepsilon_{tr} \quad (z > 0) \tag{82c}$$

Solutions of eq. (81) for which the tangential electric field is continuous at z=0 and for which the proper behavior as $z \to \pm\infty$ is obtained are

$$\tilde{\Phi}_{mn} = A_{mn}\, e^{\Gamma_{mno} z} \qquad (z < 0) \tag{83a}$$

$$= A_{mn}\, e^{-\Gamma_{mnd} z} \qquad (z > 0) \tag{83b}$$

$$\tilde{\Psi}_{mn} = \frac{B_{mn}}{\varepsilon_{tr}\Gamma_{mno}}\, e^{\Gamma_{mno} z} \qquad (z < 0) \tag{83c}$$

$$= \frac{-B_{mn}}{\Lambda_{mnd}}\, e^{-\Lambda_{mnd} z} \qquad (z > 0) \tag{83d}$$

Forcing the tangential magnetic field to be appropriately discontinuous at z=0 yields a pair of equations which may be solved for A_{mn} and B_{mn}. We readily obtain

$$A_{mn} = \frac{(jk_{xm}J_{syn} - jk_{yn}J_{sxm})\mu_o s}{(\Gamma_{mno} + \Gamma_{mnd})(k_{xm}^2 + k_{yn}^2)} \tag{84a}$$

$$B_{mn} = \frac{-(jk_{xm}J_{sxm} + jk_{yn}J_{syn})}{\left(\frac{1}{\Lambda_{mnd}} + \frac{1}{\varepsilon_{tr}\Gamma_{mno}}\right)(k_{xm}^2 + k_{yn}^2)} \tag{84b}$$

This completes the formal solution for the electromagnetic field created by the wire currents.

We now assume that in addition to the field due to the currents, there exists a "primary" field $\bar{E}_o$, given by

$$\bar{E}_o(x,y,0) = e^{-jk_{xo}x - jk_{yo}y}(E_{xo}\bar{a}_x + E_{yo}\bar{a}_y + E_{zo}\bar{a}_z) \tag{85}$$

in the plane of the interface. Furthermore, we enforce the condition that at the wire surfaces the component of electric field parallel to the wires is equal to the wire current multiplied by the wire impedance per unit length Z_w (cf. eq. (6)). Since the wire radii have been assumed small, it suffices to apply this condition at $z = -r_s$; thus we require that

$$E_x(x,qa_s,-r_s) = Z_w I_x(x,qa_s) \qquad (q = 0,\pm 1,\ldots) \tag{86a}$$

$$E_y(pa_s,y,-r_s) = Z_w I_y(pa_s,y) \qquad (p = 0,\pm 1,\ldots) \tag{86b}$$

Application of these conditions leads, after some manipulation, to the equations†

$$E_{xo} + \sum_{n=-\infty}^{\infty} (J_{sxo}T_{on} + J_{syn}U_{on})e^{-\Gamma_{ono}r_s} = Z_w a_s J_{sxo} \tag{87a}$$

$$E_{yo} + \sum_{m=-\infty}^{\infty} (J_{sxm}V_{mo} + J_{syo}W_{mo})e^{-\Gamma_{moo}r_s} = Z_w a_s J_{syo} \tag{87b}$$

in which

$$T_{on} = \frac{-1}{k_{xo}^2 + k_{yn}^2}\left[\frac{s\mu_o k_{yn}^2}{\Gamma_{ono} + \Gamma_{ond}} + \frac{k_{xo}^2}{s\varepsilon_o\left(\frac{\varepsilon_{tr}}{\Lambda_{ond}} + \frac{1}{\Gamma_{ono}}\right)}\right] \tag{88a}$$

---

†There are actually an infinite number of equations generated by the application of the wire boundary conditions, reflecting the fact that a more rigorous solution of this problem requires complete Floquet-series expansions for the wire currents [2]. However, the results thus obtained in the low-frequency limit are identical to those obtained here. One may interpret the wire boundary conditions used in this Memo, eq. (87), as

$$\int_{-a_s/2}^{a_s/2} E_x(x,qa_s,-r_s)e^{jk_{xo}x}dx = Z_w \int_{-a_s/2}^{a_s/2} I_x(x,qa_s)e^{jk_{xo}x}dx$$

and similarly for the y-directed field and current.

$$U_{on} = \frac{k_{xo}k_{yn}}{k_{xo}^2 + k_{yn}^2}\left[\frac{s\mu_o}{\Gamma_{ono} + \Gamma_{ond}} - \frac{1}{s\varepsilon_o\left(\frac{\varepsilon_{tr}}{\Lambda_{ond}} + \frac{1}{\Gamma_{ono}}\right)}\right] \quad (88b)$$

$$V_{mo} = \frac{k_{xm}k_{yo}}{k_{xm}^2 + k_{yo}^2}\left[\frac{s\mu_o}{\Gamma_{moo} + \Gamma_{mod}} - \frac{1}{s\varepsilon_o\left(\frac{\varepsilon_{tr}}{\Lambda_{mod}} + \frac{1}{\Gamma_{moo}}\right)}\right] \quad (88c)$$

$$W_{mo} = \frac{-1}{k_{xm}^2 + k_{yo}^2}\left[\frac{s\mu_o k_{xm}^2}{\Gamma_{moo} + \Gamma_{mod}} + \frac{k_{yo}^2}{s\varepsilon_o\left(\frac{\varepsilon_{tr}}{\Lambda_{mod}} + \frac{1}{\Gamma_{moo}}\right)}\right] \quad (88d)$$

Equations (87) can be manipulated into the form

$$\begin{bmatrix} E_{xo} \\ E_{yo} \end{bmatrix} = \begin{bmatrix} Z_{sxx} - T_{oo} & Z_{sxy} - U_{oo} \\ Z_{syx} - V_{oo} & Z_{syy} - W_{oo} \end{bmatrix} \begin{bmatrix} J_{sxo} \\ J_{syo} \end{bmatrix} \quad (89)$$

where

$$Z_{sxx} = Z_w a_s - \sum_{n=-\infty}^{\infty}{}' \left[T_{on} - \frac{k_{xo}a_s}{4\pi n} U_{on}\right] e^{-\Gamma_{ono} r_s} \quad (90a)$$

$$Z_{sxy} = - \sum_{n=-\infty}^{\infty}{}' \frac{k_{yo}a_s}{4n\pi} U_{on} \quad e^{-\Gamma_{ono} r_s} \quad (90b)$$

$$Z_{syx} = - \sum_{m=-\infty}^{\infty}{}' \frac{k_{xo}a_s}{4\pi m} V_{mo} \quad e^{-\Gamma_{moo} r_s} \quad (90c)$$

$$Z_{syy} = Z_w a_s - \sum_{m=-\infty}^{\infty}{}' \left[W_{mo} - \frac{k_{yo}a_s}{4\pi m} V_{mo}\right] e^{-\Gamma_{moo} r_s} \quad (90d)$$

Now the total space-averaged tangential electric field at the plane of the grid is

$$\bar{E}_{t,avg} = (E_{xo} + E_{xoo})\bar{a}_x + (E_{yo} + E_{yoo})\bar{a}_y \quad (91)$$

with

$$\begin{bmatrix} E_{xoo} \\ E_{yoo} \end{bmatrix} = \begin{bmatrix} T_{oo} & U_{oo} \\ V_{oo} & W_{oo} \end{bmatrix} \begin{bmatrix} J_{sxo} \\ J_{syo} \end{bmatrix} \quad (92)$$

so that combining eqs. (89) and (91) yields the result that

$$\bar{E}_{t,avg} = \bar{\bar{Z}}_s \cdot \bar{J}_{soo} \tag{93}$$

where the elements of $\bar{\bar{Z}}_s$ are given in eq. (90). Eq. (93) represents the relation which has been sought; it is the defining relation for the equivalent sheet impedance of the screen in the interface.

In the low-frequency limit where

$$\left|\frac{s^2}{c^2}\right| << \left(\frac{2\pi}{a_s}\right)^2$$

$$\left|\frac{s^2}{c^2}\right| << \frac{1}{\varepsilon_{tr}} \left(\frac{2\pi}{a_s}\right)^2$$

$$\left|\frac{s^2}{c^2}\right| << \frac{1}{\varepsilon_{\ell r}} \left(\frac{2\pi}{a_s}\right)^2$$

we may readily evaluate $\bar{\bar{Z}}_s$, retaining only terms of the first order in s, to obtain

$$\bar{\bar{Z}}_s = (Z_w a_s + \frac{s\mu_o a_s}{2\pi} L)\bar{\bar{I}} + \frac{a_s L \; \bar{k}_t \bar{k}_t}{2\pi s \varepsilon_o (1 + \sqrt{\varepsilon_{\ell r}\varepsilon_{tr}})} \tag{94}$$

in which $\bar{k}_t \equiv \bar{k}_{too}$ and

$$L = \ell n(1 - e^{-2\pi r_s/a_s})^{-1} \tag{95}$$

The eigenvalues of $\bar{\bar{Z}}_s$ are easily found. For perpendicular polarization,

$$Z'_s = \frac{1}{Y'_s} = Z_w a_s + \frac{s\mu_o a_s}{2\pi} L \tag{96}$$

and for parallel polarization,

$$Z''_s = \frac{1}{Y''_s} = Z_w a_s + \frac{s\mu_o a_s}{2\pi} L \left(1 - \frac{\sin^2\theta}{1 + \sqrt{\varepsilon_{\ell r}\varepsilon_{tr}}}\right)^{\dagger} \tag{97}$$

It will be noted that these results reduce to those obtained by Kontorovich [3] for the wire mesh in free space when $\varepsilon_{\ell r} = \varepsilon_{tr} = 1$. We also point out that if the dielectric medium on one side of the screen is isotropic,

† $\sin^2\theta$ may be replaced by k_t^2/k_o^2 when fields other than plane waves are considered.

with relative permittivity ε_r, then $\sqrt{\varepsilon_{\ell r}\varepsilon_{tr}} = \varepsilon_r$. This completes the development of an equivalent sheet immittance to represent the wire mesh screen in the surface of a composite laminate panel. The results may be incorporated with those obtained in the previous section, C, to obtain a complete description of the screened boron-epoxy composite panel. We discuss this point and others in the concluding section.

IV. RESULTS

A. Summary and Discussion

A.1 Graphite composite panels

A graphite composite laminate is modeled as an anistropic conductor. The anisotropy is uniaxial, the optic axis being oriented normal to the panel; the preferred directions for the conductivity are parallel to the panel surfaces. In our study of this type of composite we have assumed that the epoxy matrix essentially insulates the graphite fibers from each other, so that the conductivity in the direction normal to the panel surfaces is nil. The conductivity in the transverse direction, σ_t, is given approximately by one half the fiber conductivity multiplied by the fraction of the volume of the composite which is occupied by fibers. The permittivity in the direction normal to the laminate has been estimated in terms of the matrix permittivity, the volume fraction occupied by the fibers, and the ratio of the lamina thickness to the fiber spacing (cf. eq. (39)).

If the fibers are not insulated from each other by the epoxy matrix, then there will exist some conductivity in the direction normal to the panel, and the transverse conductivity will increase. However, it is reasonable to assume that the normal conductivity will be small in comparison to the transverse conductivity.

The connection of the tangential components of the electromagnetic field across a graphite composite panel is given by eqs. (18), (50), and (60). The connections for the two orthogonal field polarizations differ only in the shield diffusion times τ_d' and τ_d''. These are related by

$$\tau_d'' = \tau_d'(1 - \sin^2\theta/\varepsilon_{\ell r}) \tag{98}$$

and $\tau_d' = \mu_o\sigma_t d^2$. It is important to note that the precise value of $\varepsilon_{\ell r}$ is not of great importance (at least for real incidence angles θ), since it will typically be in the range $\varepsilon_{mr} - 2\varepsilon_{mr}$ and ε_m for a typical epoxy is $3.5\varepsilon_o$. Thus τ_d'' is not a strong function of θ. Furthermore, if there exists any appreciable conductivity in the direction normal to the panel, even though it is small in comparison to σ_t, then $\varepsilon_{\ell r}$ becomes effectively very large and $\tau_d'' \simeq \tau_d'$.

It is apparent that the critically important parameter for characterizing the graphite composite panel is the transverse conductivity σ_t. The conductivity of pure graphite is 7.14×10^4 mho m^{-1}. Assuming that the fibers have essentially this conductivity and that the volume fraction occupied by the fibers is 30%, we find that $\sigma_t \approx 10^4$ mho m^{-1}, which is of the order of magnitude reported in the literature [1]. An adequate model for engineering purposes of a graphite composite panel would thus appear to be a homogeneous, isotropic slab, typically 2-3 mm thick, of conductivity 10^4 mho m^{-1}.

A.2 Screened boron-epoxy composite panels

A screened boron-epoxy composite panel is modeled as an anisotropic dielectric slab with a sheet admittance in one of its surfaces. Formulas for the dyadic components of the permittivity have been derived, and an expression for the equivalent sheet impedance has been obtained. As a "worst-case" example, consider a 40-mesh screen (a_s = 0.635 mm) of stainless-steel wire ($\sigma_w = 1.1 \times 10^6$ mho m^{-1}) whose radius is 0.05 mm, and let $f = 10^8$ Hz, at the upper limit of the EMP spectrum. Then we find that the normalized screen admittance $\eta_o Y'_s$ is 1018 - j3016. Now at $f = 10^8$ Hz, $|sd/c| = 0.0063$ for d = 3 mm. Clearly, for any reasonable value of ϵ_{tr}, the effective sheet admittance of the composite panel and the screen is simply that of the screen alone; thus the electromagnetic field connection across the panel is that given by eqs. (18) and (70).

It is now evident that for electromagnetic shielding calculations the only important parameter of the composite material itself is $\sqrt{\epsilon_{tr}\epsilon_{\ell r}}$, the geometric mean of the transverse and longitudinal relative permittivities (cf. eq. (97)). We may estimate this parameter using eqs. (41) for q = 1/3, $d_\ell/a \approx 1$, assuming that $\epsilon_m = 3.5\epsilon_o$ and $\epsilon_f = 10\epsilon_o$[†]. We find for this case

$$\sqrt{\epsilon_{\ell r}\epsilon_{tr}} \approx 4.52 \qquad (99)$$

[†]The value of the permittivity of boron fibers is not known. This value was obtained by W. Gajda of Notre Dame [4], who is not yet convinced of its accuracy. Interestingly, however, it happens that for this choice of parameters, $\epsilon_{tr} = 4.58$ and $\epsilon_{\ell r} = 4.47$, so the medium is nearly isotropic.

Now the factor by which the "grid-induced" inductive terms in Z_s' and Z_s'' differ is $[1 - \sin^2\theta/(1 + \sqrt{\epsilon_{\ell r}\epsilon_{tr}})]$. In our example, variation of θ from 0° to 90° causes this factor to decrease from unity to 0.82, so the differences between Z_s' and Z_s'' are not large. We conclude that the critical parameters for the electromagnetic characterization of screened boron-epoxy composite skin panels are those of the screen itself: the wire radius and conductivity, and the mesh size.

Typical wire mesh screen parameters are as follows:

1. <u>wire material</u>: aluminum ($\sigma_w = 3.7 \times 10^7$ mho m^{-1})
   phosphor bronze ($\sigma_w = 1.1 \times 10^7$ mho m^{-1})
   stainless steel ($\sigma_w = 1.1 \times 10^6$ mho m^{-1})
2. <u>mesh sizes</u>: a_s = 0.635 mm (40 mesh)
   = 0.212 mm (120 mesh)
   = 0.127 mm (200 mesh)
3. <u>wire radii</u>: r_s = 0.127 mm (diameter = 0.010")
   = 0.051 mm (diameter = 0.004")

It is a simple matter to compute Z_s' and Z_s'' for various combinations of these parameters as functions of the frequency. Some representative curves for Z_s' for 10^5 Hz $\leq f \leq 10^8$ Hz are shown in Fig. (7).

B. Concluding Remarks

We have found in this study that of the many geometrical and electrical parameters necessary completely to characterize advanced composite materials from the electromagnetic point of view, only a few turn out to be of critical importance for the analysis of electromagnetic penetration of composite panels, at least in the EMP frequency range ($f < 10^8$ Hz). These critical parameters are

<u>for graphite composites</u>: the transverse conductivity σ_t and to a lesser extent the longitudinal permittivity ϵ_ℓ; if the conductivity normal to the laminae is appreciable, then the <u>only</u> parameter of importance is σ_t;

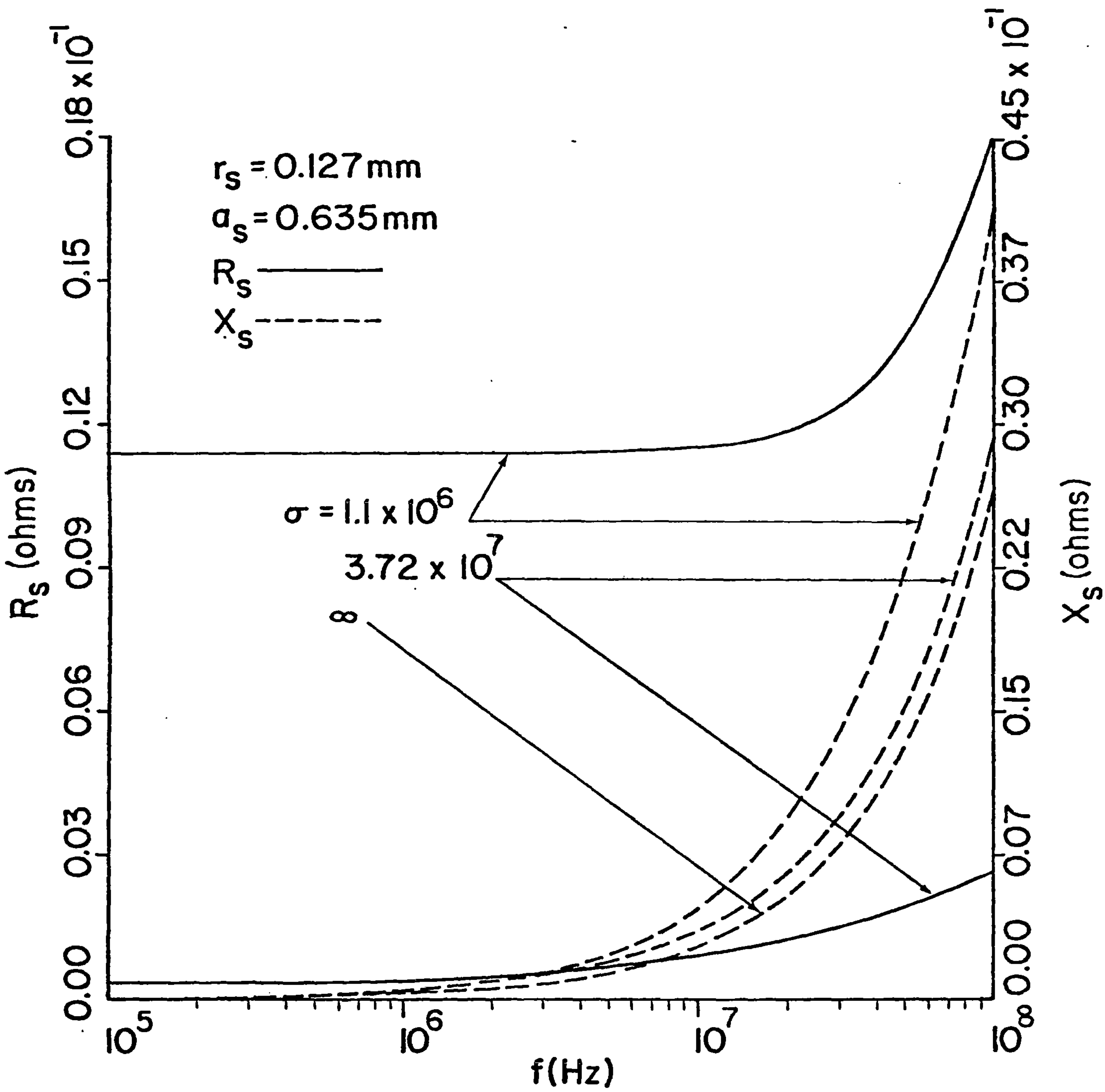

Fig. 7a. Curves of $Z_s' = R_s + jX_s$ vs. f; $r_s = 0.127$ mm and $a_s = 0.635$ mm .

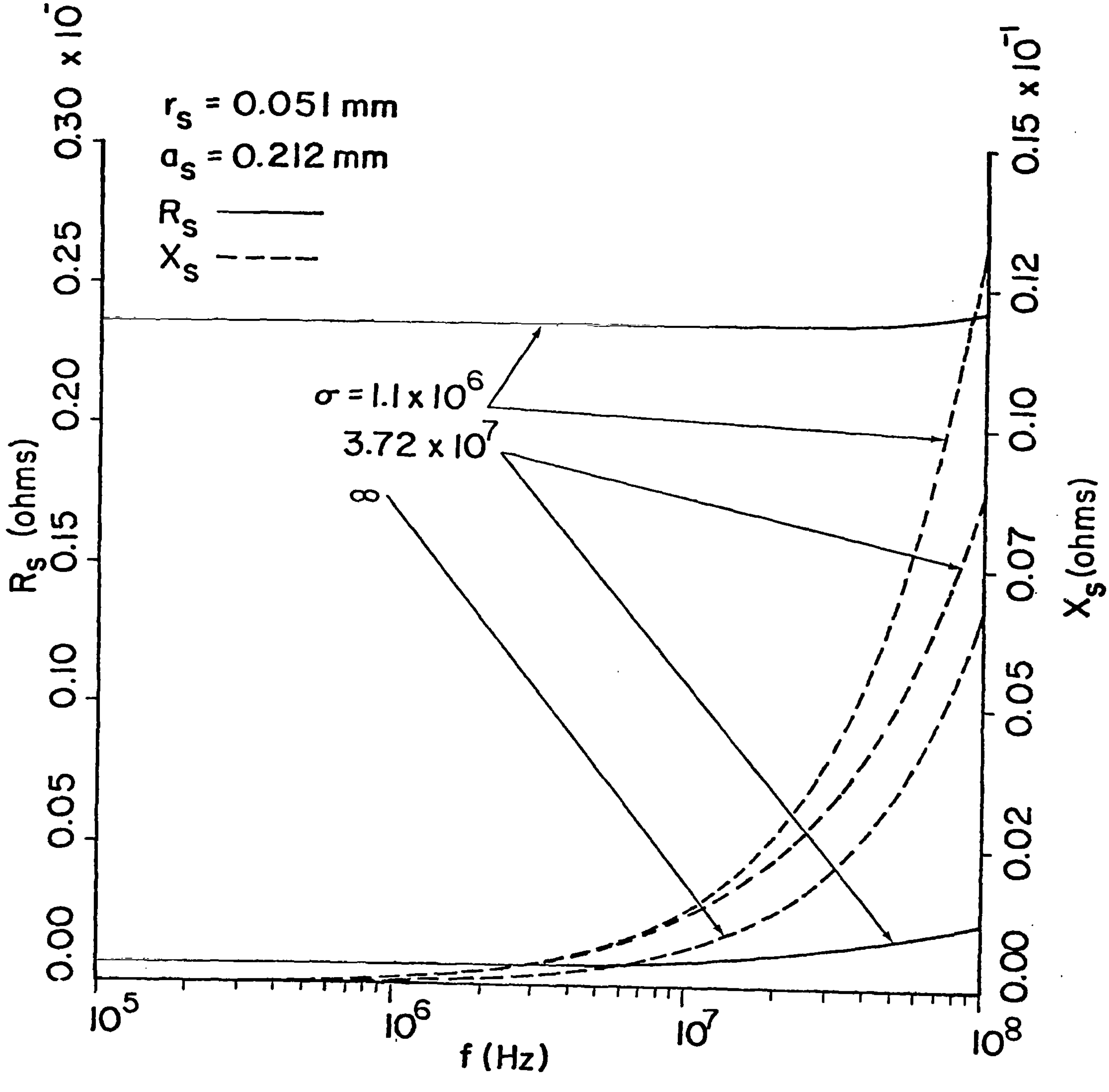

Fig. 7b. Curves of $Z'_s = R_s + jX_s$ vs. f; r_s = 0.051 mm and a_s = 0.212 mm .

for screened boron-epoxy composites: the screen parameters a_s, r_s, and σ_w and to a lesser extent the geometric mean of the transverse and longitudinal relative permittivities $\sqrt{\epsilon_{\ell r}\epsilon_{tr}}$.

It is fortunate from the standpoint of EMP protection engineering that so few of the composite parameters are necessary to treat the relevant electromagnetic field problems. This is so since, as we have previously pointed out, the study of the basic electrical properties of advanced composites is still in its infancy; consequently, available data are very sparse. However, the critical parameters σ_t and $\sqrt{\epsilon_{\ell r}\epsilon_{tr}}$ can be estimated on the basis of what limited data are now available, using analyses of the type which have been discussed in this Memo.

References

[1] L. Allen, W. F. Walker, and K. R. Siarkiewicz, "An Investigation of the Electromagnetic Properties of Advanced Composite Materials," IEEE 1976 International Symposium on Electromagnetic Compatibility Record, pp. 174-179.

[2] D. A. Hill and J. R. Wait, "Electromagnetic Scattering of an Arbitrary Plane Wave by a Wire Mesh with Bonded Junctions," Can. J. Phys., Vol. 54, pp. 353-361, 15 February 1976.

[3] M. I. Kontorovich, "Averaged Boundary Conditions at the Surface of a Grating with Square Mesh," Radio Engr. Elect. Phys., Vol. 8, pp. 1446-1454, 1963.

[4] R. Stratton, private communication.